

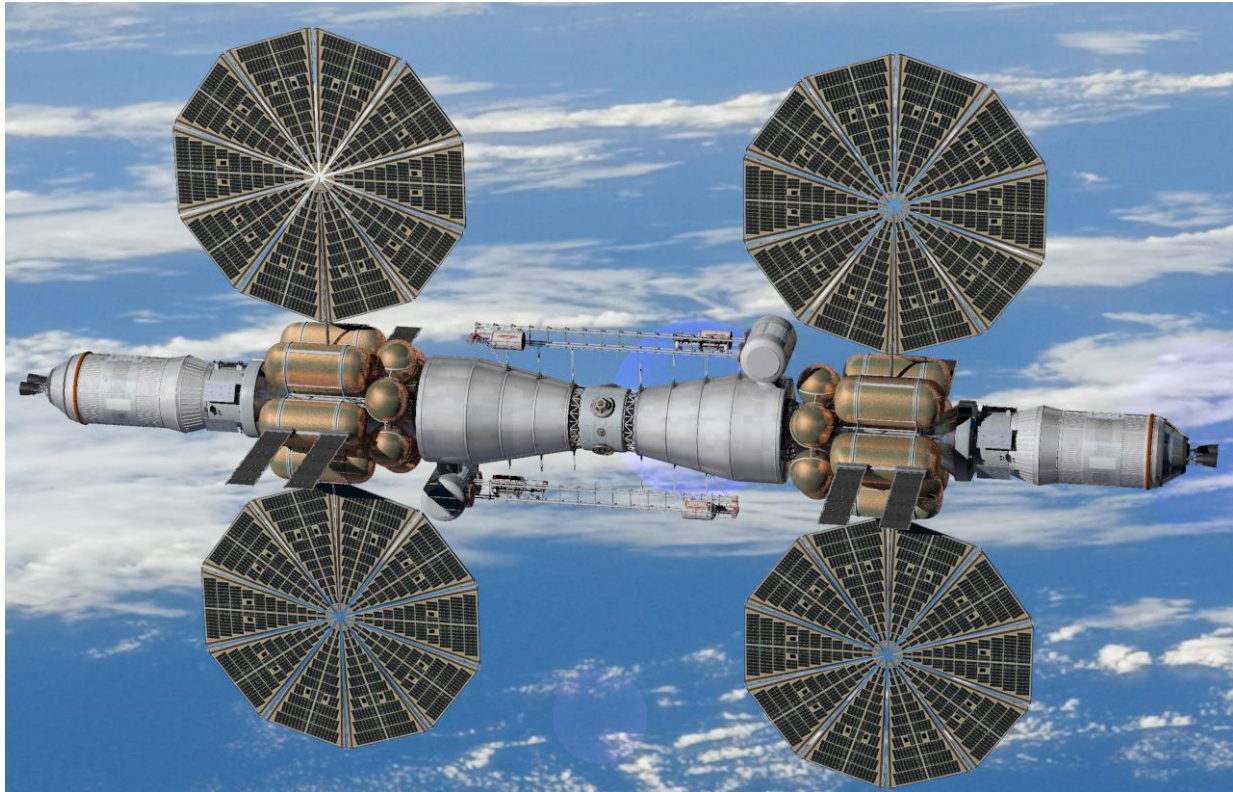
The Turbolift: Linear Sled Hybrid Artificial Gravity Concept  
NASA Innovative Advance Concepts (NIAC)  
Phase I Final Report NNX17AJ77G

Feb 14, 2018

Jason Gruber (PI)<sup>1</sup>, Kimia Seyedmadani<sup>2</sup>, and Dr. Torin K. Clark (Co-I)<sup>2</sup>

<sup>1</sup>Innovative Medical Solutions Group Laboratories, Inc.

<sup>2</sup>Smead Aerospace Engineering Sciences, University of Colorado-Boulder



## Executive Summary

Future crewed space exploration missions into deep space will require enhanced countermeasure technologies to ensure astronaut health. One such hazard is extended exposure to reduced gravity levels (i.e., microgravity, lunar gravity, or Martian gravity). Reduced gravity negatively impacts many physiological systems, leading to hydrostatic intolerance, musculoskeletal atrophy, sensorimotor impairment, bone demineralization, cardiovascular deconditioning, and visual alterations<sup>1</sup>. Various countermeasures have been employed for mitigating these effects, such as exercise, pharmaceuticals, diet, and fluid loading. However, these approaches treat individual symptoms, such that each physiological system is addressed with typically one countermeasure. An alternative to this approach is artificial gravity (AG), which promises to be a holistic, comprehensive countermeasure<sup>2</sup>. The traditional approach to creating AG is through centrifugation. However, centrifugation is not a “pure” form of AG and typically includes the drawbacks of Coriolis forces, gravity gradients, and vestibular cross-coupled illusions.

As an alternative, we have proposed a Linear Sled Hybrid (LSH) AG system to mitigate astronauts’ physiological deconditioning. This system functions by applying pure linear acceleration to produce footward loading. There is a half rotation ( $180^\circ$ ) to reorient the rider between acceleration and deceleration phases, such that the loading remains footward, as when standing on Earth. The rotation also provides some footward acceleration to the lower body through centripetal acceleration; hence the “hybrid” aspect of the design (Figure 1). At the end of the deceleration, the rider then accelerates back in the opposite direction and the sequence repeats.

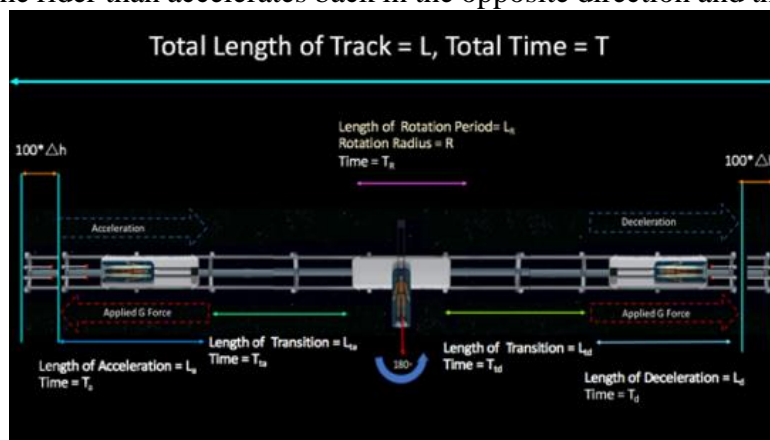


Figure 1: Linear Sled Hybrid AG system - from left to right the rider accelerates to produce footward loading, does a half rotation, then decelerates also producing footward loading and then the sequence repeats.

This proposed system could be integrated with future crewed space vehicles in a variety of manners. One approach that we have explored is for it to be added to the outside of the vehicle as a subsystem. We propose a pressurized pod to enclose the rider, which performs the sequence of motions in Figure 1. The system could utilize both sides of the track and have two pods, such that two astronauts could ride on the system at a time (Figure 2).

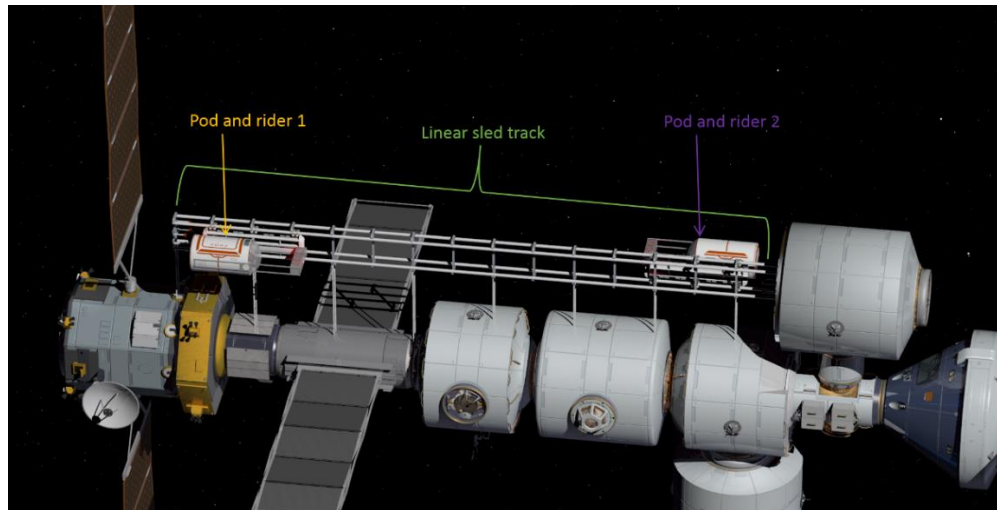


Figure 2: The LSH system with two pods integrated into an existing space habitat

The LSH AG system could broadly prove beneficial for any long-duration space exploration mission. As previously mentioned, extended duration exposure to microgravity impairs astronauts' ability to function and negatively impacts their health. Many of these deleterious effects are expected to grow with even longer duration missions than current 6-month International Space Station (ISS) stays. Furthermore, longer exposures to microgravity may uncover additional physiological concerns and interactions that have not yet been identified. For planetary landing missions to the moon or Mars, it is currently unknown whether these reduced gravity environments (0.16 and 0.38 G, respectively) will be sufficient to help mitigate or slow astronaut deconditioning. Thus, the LSH AG system may be critical to enabling crewed long-duration lunar stays, cis-lunar exploration, Mars orbital missions, exploration of Martian moons, Martian landings, or any further destination in our solar system (e.g., Europa). In the foreseeable future, we envision the LSH AG system to be directly applicable to crewed missions to Mars, which will require 1+ year of microgravity exposure, in addition to any time spent on the surface (potentially ~2 years).

There are three aspects to be considered regarding the feasibility of this system; human health benefits, human tolerability during LSH operation, and the associated cost of engineering and designing the system. Regarding the human health benefits, while AG has not been validated as a countermeasure for astronauts in space, presumably replicating 1 G would be beneficial in maintaining human health as it is here on Earth. We consider a range of different motion sequences that might prove optimal in maintaining astronaut health during long-duration exposure to microgravity.

We investigated the human tolerability of the LSH motions via simulation of the well-validated "observer" computational model of orientation perception. The motion sequence of the LSH system was found to be well-perceived with no vestibular cross-coupled illusion occurring, even if the simulated rider tilts his/her head<sup>3</sup>. Human studies have been pilot tested, assessing the potential concern of motion sickness and physical discomfort during the 180° rotation phase, which have been successful. A tolerable LSH AG system may allow for a comprehensive countermeasure for spaceflight-induced physiological deconditioning.

Mass, power, and volume, and the associated cost of the LSH system were the main design drivers for defining this concept. Total added mass was the sum of masses of the pod, actuators, and structure of rail on which the pod travels. As a preliminary estimate of the mass required for such a system, we considered the mass of the pressurized pod and performed calculations regarding the required track length. We assumed that life support for the pressurized pod would be provided from the crewed vehicle, but that the pod would need to be capable of sustaining one astronaut for a maximum of 2.5 hours at a time. This timeframe was motivated from studies demonstrating centrifuge AG of 1 hour per day to mitigate physiological deconditioning that otherwise occurs during the ground-based space flight analog of bed rest. This also compares well with the ~2 hours per day of exercise each crewmember performs on the ISS<sup>4</sup>. Accounting for some buffer time for entry/exit and contingencies, we assumed the pressurized pod would provide Environmental Control and Life Support System (ECLSS) for this time<sup>5</sup>. Using mean ECLSS requirements, an average rider, and associated systems, we estimated the required mass of the pressurized pod. The power inside of the pod was dependent on the electronics used inside such as a fan for ventilation, cabin lights, and heat removal from inside the pod. The mass of the structure was a function of the length and material used for the railing. The duration of each phase of linear acceleration/deceleration and half rotation dictated the length required. We included a margin of safety at both ends of the track to allow for a tolerable emergency stop. We explored a range of motion profiles, and present two cases studies that yielded the maximum and minimum track length in Table 1, where  $T_{a/d}$  is time spent during acceleration or deceleration,  $T_R$  is defined as the time during rotation phase,  $T_T$  is a transient time between rotation and acceleration or deceleration phase.

Table 1: Max and Min Linear Motion Profile

Case	Acceleration (m/s <sup>2</sup> )	T <sub>a/d</sub> (s)	T <sub>T</sub> (s)	T <sub>R</sub> (s)	T (s)
Max	9.81	1	1	1.67	5.67
Min	9.81	0.25	0	1.12	1.62

The mechanism of actuation of the LSH is dependent upon the profile of the motion. After determining the motion profile for the LSH, the theoretical power/energy requirements for both linear acceleration and rotation phase were computed for the structure of the LSH, the values are presented in Table 2 for the max and minimum of length, mass, and power/energy required for our design parameters. Note that some of the LSH system configurations yield a very short track length.

Table 2: Length, Mass, and Power Estimation (Pod with Counterweight and Track)

Case	Length (m)	Mass (Kg)	Power/Energy (Kw-Hr)
Max	49.47	6,871.23	12,368.53
Min	6.95	1,237.12	3,510.61

As shown in Figure 2, the LSH is attached outside of the crewed vehicle. Therefore, it would not impact the existing internal habitable volume of the vehicle. The pod design adds a small habitable volume of ~1.5 m<sup>3</sup>. This volume was designed to keep the astronaut alive for the duration of intended use (<2.5 hours).

Based upon our preliminary analysis, the LSH system appears to be a feasible approach to creating AG, which is likely to be beneficial to protecting against astronaut physiological deconditioning on a gateway spacecraft in cis-lunar space or even further away from Earth. Specifically, we found the motion sequence is likely to not be disorienting for the rider and

provided preliminary engineering analysis of the track length, and pod in terms of mass, power, volume, and monetary cost.

Future work should further refine estimates for the LSH system's mass, power, and volume, as well as provide a cost analysis. Human testing can further verify the system, particularly the 180 degree rotation, is tolerable in terms of motion sickness and physical comfort. It can also help inform the required length of the rotation phase. Finally, future work should aim to demonstrate the system indeed mitigates physiological deconditioning that otherwise occurs in microgravity. However even at this point there is strong reason to believe replicating gravity through the LSH AG system will be beneficial for astronaut health.

## Table of Contents

<b>EXECUTIVE SUMMARY .....</b>	<b>2</b>
<b>INTRODUCTION AND BACKGROUND.....</b>	<b>8</b>
PHYSIOLOGICAL DECONDITIONING DUE TO MICROGRAVITY.....	8
ARTIFICIAL GRAVITY BACKGROUND .....	8
LINEAR SLED HYBRID AG CONCEPT .....	9
<b>CONCEPTUAL DESIGN OF THE LINEAR SLED HYBRID SYSTEM.....</b>	<b>10</b>
LSH MOTION PROFILE: .....	10
<i>Potential for Rider Disorientation during LSH Motions:</i> .....	18
SUBSYSTEM ARCHITECTURE: .....	21
<i>Linear Track Design</i> .....	21
<i>Environmental Control and Life Support Systems (ECLSS)</i> .....	25
<i>Actuation Subsystem</i> .....	30
<i>Cost Estimate for the LSH Concept:</i> .....	31
RISK ASSESSMENT AND FAILURE MODE AND EFFECTS ANALYSIS.....	32
<b>SUMMARY OF FEASIBILITY .....</b>	<b>34</b>
INTEGRATING INTO FUTURE MISSION CONCEPTS .....	34
INTEGRATING INTO PLANETARY MISSIONS .....	35
FUTURE WORK .....	36
<b>PUBLICATIONS.....</b>	<b>37</b>
OUTREACH AND PUBLIC ENGAGEMENT .....	37
<b>ACKNOWLEDGEMENTS .....</b>	<b>37</b>
<b>LIST OF ACRONYMS.....</b>	<b>38</b>
NOMENCLATURE .....	38
<b>REFERENCES.....</b>	<b>40</b>
<b>APPENDIX.....</b>	<b>42</b>
MASS AND POWER CALCULATION FOR OVERALL THE LSH SYSTEM: .....	42
POWER FOR ONE-CYCLE LMP 2: .....	43
RISK DEFINITIONS.....	44
RISK DATA BASE .....	45

**Table of Figures**

Figure 1: Linear Sled Hybrid AG system ..... 2  
 Figure 2: The LSH system with two pods integrated into an existing space habitat ..... 3  
 Figure 3: Radius of rotation with respect to the center of mass..... 12  
 Figure 4: Net acceleration applied at center of mass ..... 13  
 Figure 5: Acceleration rotation (ar), Constant rotation (cr) and Deceleration rotation (dr) sub-phases of the rotation phase ..... 14  
 Figure 6: Rotation Motion Profiles ..... 15  
 Figure 7: Acceleration Applied to Human..... 16  
 Figure 8: Observer Model Simulation ..... 19  
 Figure 9: Pod Subsystem Design Concept Decision Diagram..... 21  
 Figure 10: Pod and the Counter Weight ..... 26  
 Figure 11: Pod Dimension ..... 26  
 Figure 12: Pressures Applied to the Wall of Pod..... 26  
 Figure 13: Human O<sub>2</sub> and CO<sub>2</sub> Balance ..... 28  
 Figure 14: Pod Mass Trend by Adding Radiation Shield..... 29  
 Figure 15: 1/20th scale model of the guide track actuation approach ..... 31  
 Figure 16: Power for one-cycle for LMP 2..... 43

**Table of Tables**

Table 1: Max and Min Linear Motion Profile ..... 4  
 Table 2: Length, Mass and Power Estimation (Pod with Counter Weight and Track) ..... 4  
 Table 3: Various Cases with Different Durations of Each Phase ..... 12  
 Table 4: Motion Profile - Rotation..... 14  
 Table 5: Motion Profile and Number of Cycle per Hour..... 23  
 Table 6: The length of the track and estimated mass and power required for various LSH configurations ..... 23  
 Table 7: ECLSS Input and Output for a Crew Member (Cm)..... 25  
 Table 8: Gas Composition inside Pod at Start ..... 27  
 Table 9: Mass and Power of Pod ..... 30  
 Table 10: Cost Estimate Model- Cost Calculated in Million Dollars..... 32  
 Table 11: Identified Risk and Mitigation..... 32  
 Table 12: FMEA Analysis for Turbolift NIAC Phase I..... 33  
 Table 13: Total Mass, Power and Cost of The LSH (Pod, Counter weigh and Track) ..... 34

## Introduction and Background

### Physiological Deconditioning Due to Microgravity

Future human space exploration is limited by the physiological deconditioning astronauts experience as a result of long-duration microgravity or reduced gravity exposure<sup>1</sup>. Long-duration exposure to microgravity leads to bone loss, muscle atrophy, cardiovascular deconditioning, and visual degradation. During gravity transitions astronauts experience sensorimotor impairment. This is not an exhaustive list of physiological concerns, and additional forms or variants of deconditioning may occur with increased mission duration. These various physiological concerns are thought to result from the lack of gravitational loading typically experienced here on Earth. These deleterious effects threaten astronaut safety, performance, and long-term well-being.

Various countermeasures have been employed for mitigating these effects, such as exercise, pharmaceuticals, diet, and fluid loading. However, these approaches treat individual symptoms – each physiological system is addressed with primarily one countermeasure. Furthermore, the current suite of countermeasures has been only partially effective and may be insufficient for longer duration, exploration missions. An alternative is artificial gravity (AG), which promises to be a holistic, comprehensive countermeasure<sup>2</sup>. Here, we propose and perform preliminary analysis to assess the viability of a novel AG concept: the linear sled “hybrid” (LSH) approach. LSH involves repeatedly linearly accelerating and decelerating the astronaut (Figure 1) to replicate the gravitational loading otherwise missing in microgravity. We note that, in addition to the physiological deconditioning resulting from reduced gravity exposure, astronauts are also threatened by elevated radiation exposure. The LSH system is not intended to be a countermeasure against radiation exposure.

### Artificial Gravity Background

AG systems are a promising potential countermeasure for physiological deconditioning due to microgravity. While an AG system has not yet been validated in space as a human countermeasure<sup>2</sup>, conceptually it is reasonable to suspect that replicating the gravitational loading we experience here on Earth would be beneficial.

AG designs typically utilize centrifugation. In this approach, loading from sustained centripetal acceleration (or centrifugal force) is created through off-axis rotation at a constant rate<sup>3</sup>. An example of the force from centripetal acceleration is that which keeps water in a bucket that is being spun around on a string. The resulting force from centripetal acceleration is proportional to the radius of rotation and the square of the rotation rate. Practical centrifuge designs typically involve a shorter radius. Thus to produce a desired centripetal acceleration level (e.g., 1 Earth G or  $9.81 \text{ m/s}^2$ , though other levels may be appropriate), a fast rotation rate is required. The shorter radius and/or higher rotation rate causes three challenges to person on the spinning centrifuge: 1) the vestibular cross-coupling illusion (i.e., Coriolis illusion) when out-of-plane head movements are made, which is highly disorienting and leads to motion sickness, 2) unexpected Coriolis forces when the limbs or body translate, and 3) a gravity gradient, in which the gravitational loading increases from head to foot with increasing effective radius. These confounds may make centrifuge AG less tolerable for human riders.

### Linear Sled Hybrid AG Concept:

As an alternative AG design, we have proposed a linear sled “hybrid” system, shown in Figure 1. Here, the AG is produced primarily through “pure” linear acceleration. A brief acceleration phase creates footward gravitational loading, shifting body fluid toward the rider’s feet and providing weight bearing to the legs/feet, as if the rider were standing on Earth. Then the astronaut is quickly rotated 180° to reorient the rider, during which he/she continues to translate at a constant linear velocity. Next the rider is linearly decelerated, again creating footward gravitational loading. The astronaut is then accelerated back in the opposite direction, repeating the sequence. Between the acceleration/deceleration phases and rotation phase, we have accounted for transition phases in which the rider only linearly translates at a constant velocity (however some designs have removed these transition phases).

During the acceleration and deceleration phases, uniform gravitational loading (e.g., 1 Earth G) will be applied across the entire body (no gravity gradient). Furthermore, as there is no rotation, there will presumably not be any vestibular cross-coupled illusion or Coriolis forces. In this sense, the linear acceleration and deceleration of the LSH provides a “pure” form of AG.

During the 180° rotation, there will also be AG loading due to centripetal acceleration, hence the “hybrid” aspect of combining linear and centripetal acceleration. We envision the rotation occurring about an axis located at the rider’s head (though other configurations are feasible). This has the advantage of simplifying the motion stimulation to the vestibular system, located in the rider’s head (i.e., only rotational stimulation at this location, roughly at the glabella). It also causes the loading from the centripetal acceleration to be exclusively footward. We note that the loading during the 180° rotation would have a gravity gradient. There would be no centripetal acceleration at the rider’s head (radius of rotation=0), but there would be substantial loading at their feet (radius  $\approx$  height of rider). Similarly, there would be Coriolis forces if the rider moves his/her limbs, particularly during the peak of the rotation. However, one would not expect any vestibular cross-coupled illusion if the rider makes head movements, even during the rotation, because the rotation is not sustained like on a centrifuge. Lastly, we note that during the beginning and ending of the 180° rotation, where there is angular acceleration/deceleration, lower portions of the rider’s body would experience tangential accelerations which would be perpendicular to the rider’s longitudinal axis.

In summary, the LSH AG system will provide longitudinal, footward loading to the astronaut rider’s body while in space. This is expected to mitigate the physiological deconditioning that occurs in microgravity by replicating the gravity loading here on Earth.

There are two important temporal aspects to the LSH system that should be noted. First, we envision astronauts to not be continuously exposed (i.e., 24 hours per day) to the repeated LSH motion sequence. Instead, each astronaut may ride on the LSH system on the order of 1 hour per day (experiencing hundreds to a few thousand repeated motion sequences depending upon the duration of each sequence). This is typically referred to as “intermittent” AG<sup>2</sup>. While it remains to be validated with astronauts in space, ground studies using long-duration head down tilt bed rest as a microgravity analog have demonstrated such intermittent centrifuge AG to be beneficial in mitigating the physiological deconditioning otherwise experienced. It is logical to believe the

loading from the LSH system would be similarly beneficial, even if only experienced intermittently (i.e., approximately 1 hour per day).

Second, the LSH has another, much faster temporal aspect in that the loading changes during each phase (acceleration, transition, rotation, transition, deceleration). We refer to this as the “duty cycle” of the LSH AG system to capture the higher frequency, repeated sequence of the loading profile. Some recent research suggests that musculoskeletal strength benefits from higher frequency, impact loads (e.g., those experienced while walking, running, and jumping here on Earth) as opposed to constant loading (e.g., those from standing still). Thus the onset and offset of loading between phases of the LSH system may actually prove to have physiological benefits vs. constant, sustained loading that would be experienced on a centrifuge.

## Conceptual Design of the Linear Sled Hybrid System

### LSH Motion Profile:

The conceptual motion profile of the LSH system is shown in Figure 1. However, there remain aspects of the design to be quantified. Specifically, we aim to consider: 1) the duration of each phase, 2) the loading during the acceleration and deceleration phases, and 3) the profile of the 180 degree rotation. Selecting these design parameters requires trading off engineering demands (and associated size and cost), efficacy of the LSH system in mitigating astronaut deconditioning, and the tolerability to the rider. We emphasize that there is currently little to no physiological data to help inform these design decisions. Thus, we have taken an approach of considering a range of reasonable designs and evaluating each in terms of the engineering demands (e.g., track length, etc.).

We begin by considering the duration of each phase of the LSH sequence with regards to the efficacy in mitigating physiological deconditioning. In selecting durations of each phase, one might consider the “duty cycle” of acceleration loading during the repeated sequence (i.e., what portion of the repeated sequence does the astronaut experience longitudinal loading). Longer durations for the linear acceleration and deceleration phases would provide a higher duty cycle, and thus a closer replication of the continuous loading experienced here on Earth. The constant velocity phases provide no gravito-inertial loading (i.e., the astronaut would feel weightless during these phases, as normally in microgravity) and thus these phases are likely not beneficial for mitigating physiological deconditioning. However, as noted above, the dynamic impacts during transitions between non-loading and loading phases may actually be helpful for musculoskeletal health. The rotation phase provides centripetal acceleration loading, but it is not “pure” AG, in that there will be gravity-gradients and tangential accelerations. Thus, from the standpoint of providing loading to mitigate astronaut physiological deconditioning, it would be preferable to have longer duration acceleration and deceleration phases, very short or no transition phases, and a relatively short rotation phase.

However, from an engineering design standpoint, presumably a shorter track length would be preferable to reduce mass and thus cost. From this perspective, shorter durations for all phases are preferred. This is particularly critical for the acceleration/deceleration phases, in which longer durations not only increase the track length associated with those phases, but lead to a higher linear

translation velocity for the transition and rotation phases which further extends the required total track length.

Finally, we consider what may be tolerable for the human riders. Presumably, any duration of acceleration/deceleration would be tolerable as humans regularly experience continuous G-loading just standing on Earth, as well as very brief G-loading (for example jumping on a trampoline). We suggest a longer duration for the 180 degree rotation (and thus slower rotation speed) may be preferable in terms of rider comfort and susceptibility to motion sickness. How short/fast of a rotation becomes intolerable is unknown and remains a critical area for future human testing. We note that tilting one's head back and forth fairly quickly (e.g. at 1 Hz) would produce similar motion stimulation to the vestibular system in the head and generally does not induce motion sickness for most people. This suggests fairly short durations for the 180 degree rotation may be tolerable. Yet, tilting one's own head may be different than full body, passive rotations on the LSH system. Finally, it may be beneficial in terms of tolerability to have longer transition durations between acceleration/deceleration and rotation, but this has not been verified with testing.

Second, we consider the loading during the acceleration/deceleration periods. In terms of efficacy in mitigating physiological deconditioning, presumably 1 G would be sufficient since it replicates that which is normally experienced here on Earth. However, there is not yet physiological data verifying this in spaceflight or a ground-based analog. It may also be possible that less than 1 G is sufficient or that greater than 1 G is even more effective, particularly since given the "duty cycle" of the loading and the proposed intermittent use of the LSH system. Specifically, 1 hour of 60% duty cycle of 1 G loading may not replicate continuous 1 G loading of Earth (though in studies using bed rest as a spaceflight analog, ~1 hour of 1 G centrifuge AG appears to be highly beneficial). If necessary, 1 hour of 60% duty cycle of, for example, 2 G loading might be fully mitigating.

Finally, for a mission in which astronauts spend time on the Martian surface it may actually be best to match this level and create 0.38 G loading to prepare for this environment. This lower G-level may or may not be sufficient for maintenance of musculoskeletal or other physiological systems, but is conceptually appropriate for the neurovestibular/sensorimotor system, in which prior exposure to a novel environment is typically beneficial (though we note that 0.38 G with a duty cycle does not perfectly mimic continuous 0.38 G, like on the Martian surface).

At this point, it is unknown what "duty cycle" and/or "G-level" would be sufficiently beneficial or optimal, so we therefore consider a range of cases. Specifically, we considered various lengths of each phase (Cases #1-3 in Table 1). We also consider cases with the magnitude of the linear acceleration/deceleration matching either Earth gravity (i.e.,  $9.81 \text{ m/s}^2$ ) or Martian gravity ( $3.71 \text{ m/s}^2$ , Case #4 in Table 3). Of course, there are an unlimited combination of cases that could be considered, but these were selected to span a range of reasonable design options.

Table 3: Various Cases with Different Durations of Each Phase

Case#	Acceleration (m/s <sup>2</sup> )	T <sub>a</sub> (s)	T <sub>ta</sub> (s)	T <sub>R</sub> (s)	T <sub>td</sub> (s)	T <sub>d</sub> (s)
1	9.81- Earth gravity	1	1	TBD	1	1
2	9.81- Earth gravity	1	0	TBD	0	1
3	9.81- Earth gravity	0.25	0	TBD	0	0.25
4	3.711- Mars gravity	1	0	TBD	0	1

In Table 3, T<sub>a</sub> is the duration of acceleration, T<sub>ta</sub> is the transition duration between the linear acceleration to the rotation phase, T<sub>R</sub> is duration of 180 degree rotation (determined below), T<sub>td</sub> is the transition duration between the rotation and the deceleration phases, T<sub>d</sub> is the period of deceleration, and T is the total time of one sequence on the LSH. In the remainder of this report, we focus on cases #1-3. We only consider case #4 in our assessment for a planetary mission (see Integrating into a Planetary Mission section below).

Thirdly, we consider the profile of the 180 degree rotation phase. This profile has a few constraints; it must rotate exactly 180 degrees and it must begin and end with 0 deg/sec of angular velocity (as the subsequent transition and linear acceleration/deceleration phases have no angular motion). Thus, we can break that rotation phase down into three sub-phases: an angular acceleration sub-phase, a constant angular velocity sub-phase, and an angular deceleration sub-phase. We assume the angular acceleration and angular deceleration sub-phases occur over the same duration (though asymmetric profiles could be used as well). As mentioned earlier, we assume the rotation occurs about an axis located at the rider’s head, specifically around the eye/ear location<sup>4</sup> (this distance is defined as D in Figure 3). During the rotation there will be centripetal acceleration loading that varies spatially along the rider’s body (gravity gradient) and temporally as the angular velocity of rotation increases and then decreases. Notably, the centripetal acceleration loading at the rider’s center of mass location (Figure 3) is what determines how much loading “weight” will need to be supported by the legs/feet.

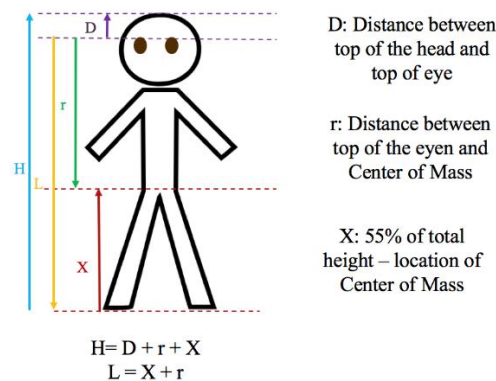


Figure 3: Radius of rotation with respect to the center of mass

In addition to loading from centripetal acceleration, there is also loading from tangential acceleration due to the angular acceleration and deceleration of the loading profile. This also varies as a function of time during the rotation profile and location along the rider’s body. Figure 4 shows

the inertial forces resulting from these accelerations and how they vary along the rider's body and over the course of the LSH motion sequence.

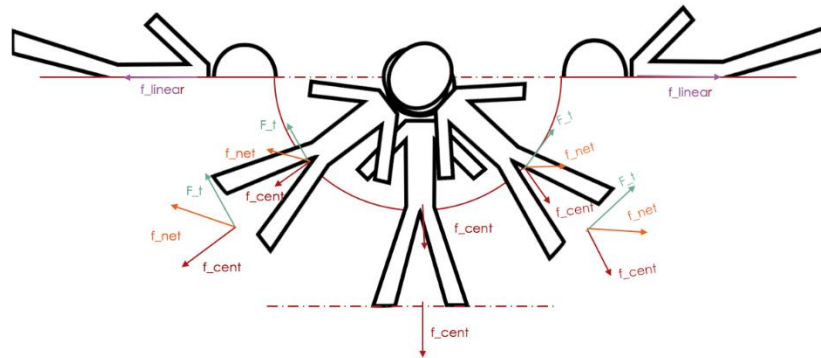


Figure 4: Net acceleration applied at center of mass

While the inertial forces from linear acceleration/deceleration ( $f_{linear}$ ) are constant during those phases and throughout the body, the inertial forces from centripetal acceleration ( $f_{cent}$ ) are larger near the feet and are maximum at the peak angular velocity (i.e., in the middle of the rotation profile). The inertial forces from tangential acceleration ( $F_t$ ) also are larger near the feet, but are maximum during the angular acceleration and deceleration sub-phases and are zero (non-existent) during the middle of the rotation when there is constant angular velocity. During the rotation, the inertial forces from tangential acceleration and centripetal acceleration combine to yield a net inertial force ( $f_{net}$ ) which is not aligned with the body's longitudinal axis during the angular acceleration/deceleration sub-phases.

While any rotation profile might be considered, we propose a few additional constraints that may be desirable. First, it is preferable for the tangential acceleration to be small, such that the net inertial force is more closely aligned with the body longitudinal axis during the angular acceleration/deceleration sub-phases. As the magnitude of the tangential acceleration is proportional to the angular acceleration/deceleration, it is desirable for the angular acceleration/deceleration to be small. Second, we propose that it may be beneficial for the loading from centripetal acceleration at the rider's center of mass to match the loading during the linear acceleration/deceleration periods. This would produce a more consistent load which must be supported by the rider's legs/feet (i.e., 1 Earth G or  $9.81 \text{ m/s}^2$  for Cases #1-3 in Table 1).

Of course, the centripetal acceleration at the rider's center of mass varies during the rotation phase and must be zero at the beginning and end of this phase (since the angular velocity must begin and end at zero, as noted above). Instead, we propose to constrain the centripetal acceleration at the rider's center of mass (at least during the peak angular velocity of the rotation phase) to match that during the linear acceleration/deceleration phase (e.g.,  $9.81 \text{ m/s}^2$ ). Given these constraints, we can define the portion of the total rotation duration in which the angular acceleration occurs (Figure 5) and then solve for all aspects of the rotation profile and the associated loading.

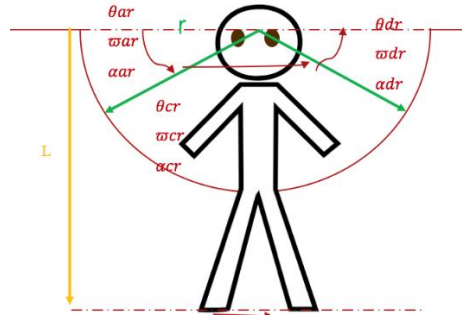


Figure 5: Acceleration rotation (ar), Constant rotation (cr) and Deceleration rotation (dr) sub-phases of the rotation phase

Table 2 shows a few different Cases (A-D) for how the rotation profile might be defined. For example, Case A uses 25% of the rotation duration for angular acceleration ( $T_{ar}$ ) and 25% for angular deceleration ( $T_{dr}$ ). Thus 50% remains for constant angular velocity rotation ( $T_{cr}$ ). To produce 1 Earth G ( $9.81 \text{ m/s}^2$ , matching the linear acceleration/deceleration in Cases #1-3 of Table 1) at the rider’s center of mass during the constant angular velocity sub-phase of rotation, yields 1.1161 seconds for the full rotation phase. (These calculations assume the rider to be 1.77m tall, with a center of mass 55% up from the feet, and an eye/ear location 0.1m below the top of the head. A rider with different anthropometry would experience a slightly different centripetal acceleration level at his/her center of mass.) Alternatively, Case C is the limit where the matched centripetal acceleration at the rider’s center of mass is only obtained for an instant and the full first half of the rotation is angular acceleration and the second half is angular deceleration, which yields a total rotation duration of 1.6743 seconds.

Table 4: Motion Profile - Rotation

Case	$T_{ar}$ or $T_{dr}$ [s]	$T_{cr}$ [s]	$T_R$ [s]
A	$0.25 * T_R$	$0.5 * T_R$	1.1161
B	$0.3 * T_R$	$0.3 * T_R$	1.2683
C	$0.5 * T_R$	0	1.6743
D	$0.42 * T_R$	$0.16 * T_R$	1.4433

The equations that are used to calculate the rotation profiles and total rotation durations are provided below.

Equation 1: the set of the equations governing the rotation profile and associated accelerations

$$\omega_{cr} = \sqrt{\frac{a_{cent}}{r}} \text{ [degree/s]}$$

$$\omega_{cr} = \alpha_{ar} * t_{ar} + \omega_{ar} \text{ [degree/s]}$$

$$\theta_{cr} = \omega_{cr} * t_{cr} \text{ [degree/s]}$$

$$\omega_{cr}^2 - \omega_{ar}^2 = 2 * \alpha_{ar} * \theta_{ar}$$

$$\theta_{ar} + \theta_{cr} + \theta_{dr} = 3.1416 \text{ [rad]}$$

$$a_{cent} = r * \omega^2 \text{ [m/s}^2\text{]}$$

$$a_{tan} = L * \alpha \text{ [m/s}^2\text{]}$$

$$\alpha = \omega \text{ [rad/s}^2\text{]}$$

Using these equations, the profile (angle, angular velocity, and angular acceleration) are shown in Figure 6. Note that when the angular acceleration/deceleration sub-phases are shorter (e.g., Case A), the magnitude of the angular acceleration/decelerations must be higher (in Figure 6, larger minimum and maximums in the bottom panel of Case A, compared to bottom panel for Case C). However, the portion of the rotation phase in which there is constant angular velocity is longer (in Figure 6, longer plateau in the middle panel for Case A compared to no plateau for Case C).

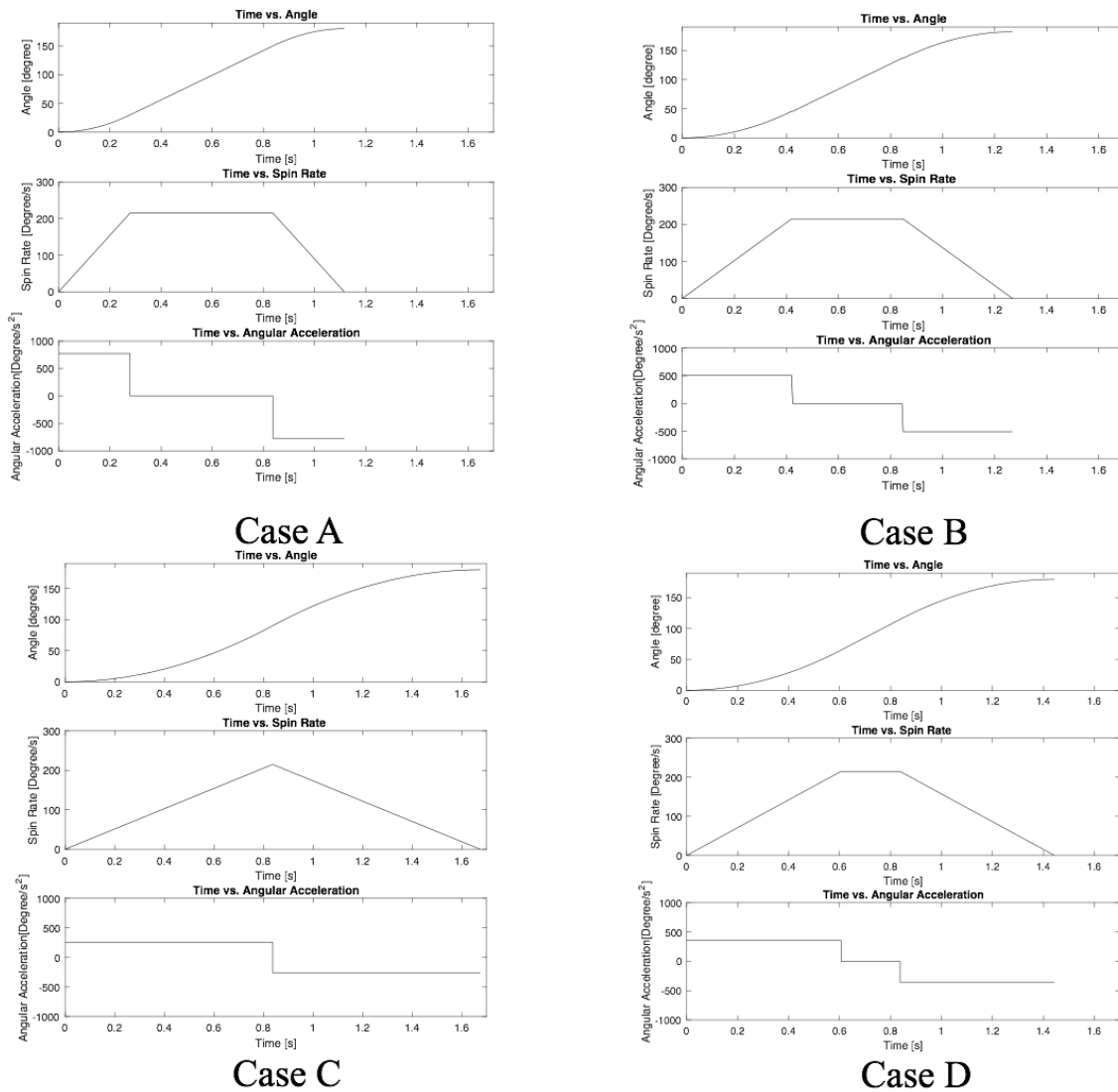


Figure 6: Rotation Motion Profiles

These different rotation profiles have important implications for the loading from centripetal acceleration and that from tangential acceleration (Figure 7). Specifically, when the angular acceleration sub-phases are shorter (Case A), the centripetal acceleration at the center of mass (which is aligned with the body longitudinal axis) matches that from the linear acceleration and deceleration for a larger portion of the rotation. However, the tangential acceleration (which is perpendicular with the body longitudinal axis) has a larger magnitude (in Case A, nearly 10 m/s<sup>2</sup>

at the rider's center of mass). While matching the centripetal acceleration for a larger portion of the rotation is presumably desirable (creating a more sustained loading throughout the LSH motion profile), the higher peak tangential acceleration is presumably undesirable. Since the tangential acceleration is perpendicular to the body longitudinal axis, it is not beneficial in replicating the axial loading when standing upright on Earth. Furthermore, larger tangential accelerations may be uncomfortable and even lead to impact injuries. Finally, note that both the centripetal acceleration magnitudes and tangential acceleration magnitudes are larger at the rider's feet compared to the center of mass, since the effective radius of rotation is longer.

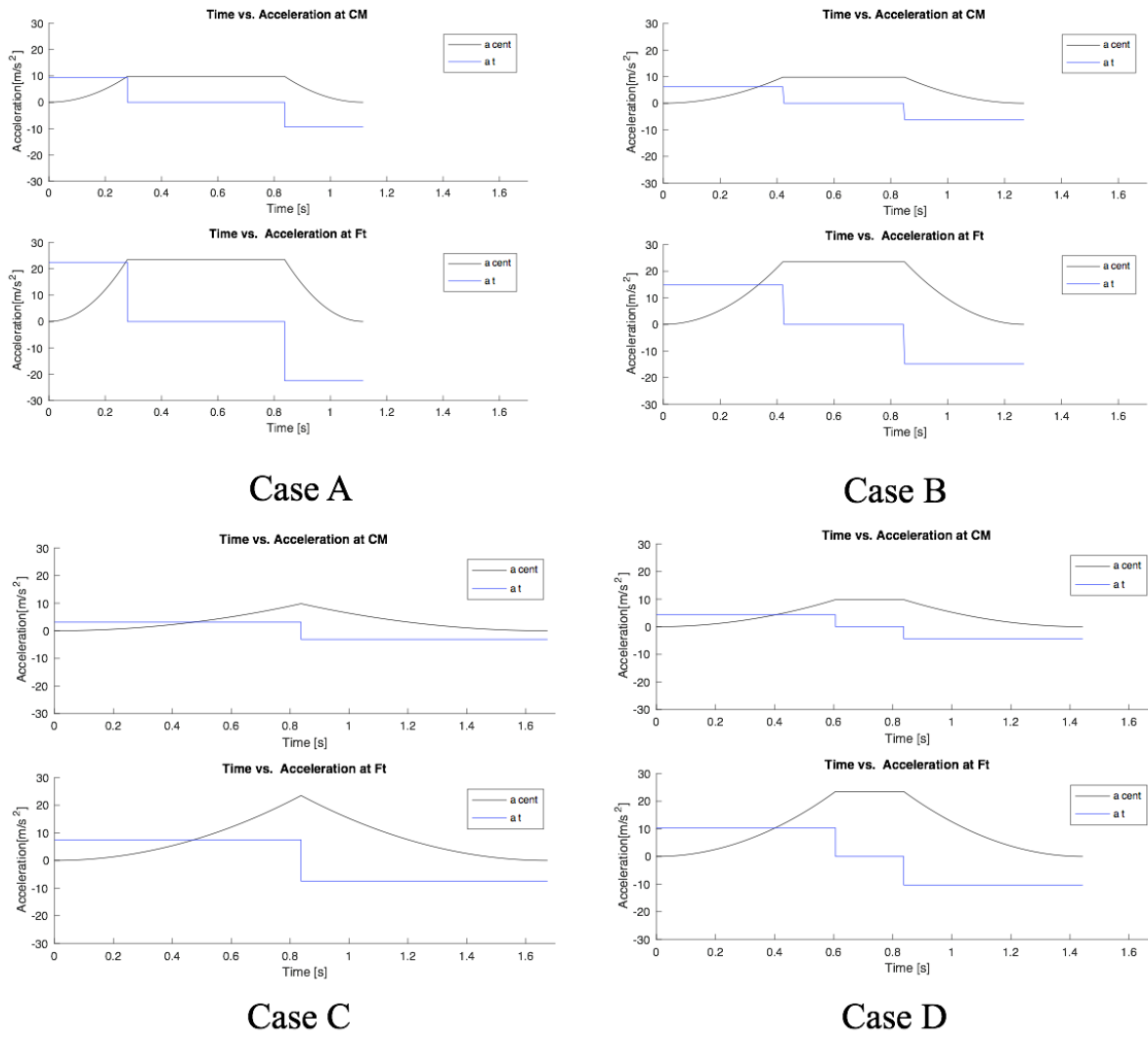


Figure 7: Acceleration Applied to Human

Case D in Figure 7 is a potentially reasonable tradeoff in keeping the peak tangential acceleration less than  $5 \text{ m/s}^2$  at the rider's center of mass, while otherwise maximizing the portion of the rotation in which the centripetal acceleration at the center of mass is  $9.81 \text{ m/s}^2$ . However, further investigation is required to determine and validate the optimal rotation profile.

Up until this point we have focused on the rotation profile (i.e., the angular velocity vs. time), however we have ignored the *axis* of this rotation relative to the rider. Figure 1 show the

rider rotating about their roll axis (i.e., an axis that goes out the rider's nose, or naso-occipital). This would be the type of head rotation experienced when tilting one's ear down towards the shoulder.

An alternative is that the rider could be "on their side" in Figure 1 and thus could rotate about their pitch axis (i.e., an axis that goes through the rider's ears, or inter-aural). This would be the type of head motion experienced when nodding one's head forward and backward to signal "yes". Of course, any combination of roll and pitch would also be physically feasible. For example, if the rider was aligned at 45 degrees and rotated about that axis, it would include some rotation in the roll and pitch axes.

At this point it is unknown which axis of rotation is preferable. We note that whatever rotation axis is used, the loading during the acceleration/deceleration, as well as that from centripetal acceleration during the rotation phase, would always be aligned with the body's longitudinal axis. This serves the purpose of replicating the direction of gravity when standing upright and thus should be equally effective in mitigating physiological deconditioning. However, one axis of rotation may prove to be preferable in terms of tolerability for motion sickness and physical comfort. Ground testing of human responses to repeated rotations will be useful in determining the preferred rotation axis.

Intertwined in the issue of preferred rotation axis is whether it is preferred to keep the direction of rotation the same or to alternate between successive LSH motion sequences. For example, in the left to right LSH motion sequence of Figure 1, the roll rotation is in the counterclockwise direction. When translating back from right to left, the next roll rotation could continue in the counterclockwise direction, completing a full 360 degree rotation. Alternatively, it could rotate back in the clockwise direction, sweeping through the same space as the prior rotation, just in the opposite direction.

Alternating vs. continuing the direction relates to the rotation axis due to potential asymmetries in motion perception and susceptibility to motion sickness. There are typically no asymmetries in the roll axis; roll rotations to the right vs. left are similarly provocative and thus if the roll axis is selected it likely does not make much difference in terms of tolerability whether rotations continue in the same direction or alternate directions. However, there is evidence of an asymmetry in perception of pitch rotation and associated susceptibility to motion sickness. Motions that correspond to pitching backwards (i.e., nose up) are typically more provocative, potentially because this corresponds to "falling backwards" which our anatomy makes us less capable of reacting to and recovering from. Thus if the pitch axis were selected, it may be preferred for the rider to always rotate by pitching forward, and thus it would be important to continue each rotation in the same direction, sweeping out full 360 degree rotations. (As an added complexity, we note that "falling forward" vs. "falling backward" is typically considered when tripping and thus rotating about the feet, causing the head to translate substantially. In the LSH rotation profile where the rotation axis is located at the rider's head and the feet swing "beneath" them, this asymmetry may differ.) Again, ground testing of human responses would be highly informative for the design of the rotation phase of the LSH system.

Finally, we note there are potential engineering advantages in how the rotation is performed. Alternating the direction of rotation each time means that the same physical space is

swept out during the sequence going from left to right vs. right to left. If the entire system is enclosed, this approach helps reduce the required pressurized volume since the module would not need to include space for the other rotation area (though see Design of a Pressurized Pod section below). On the other hand, depending upon the actuation mechanism, it may be more or less difficult to create rotations in the same vs. alternating directions (see the Actuation Subsystem section). Finally, if the LSH system is attached to the primary spacecraft habitat, each rotation will impart a torque on the habitat. Alternating the rotation direction may be beneficial for countering each previous torque, though a counter rotating mass could also be used to negate the torques applied to the habitat.

### **Potential for Rider Disorientation during LSH Motions:**

One concern for feasibility of the LSH system is that stimulation patterns are unique and may be disorienting for the rider. As a preliminary assessment of the feasibility of such a system, we aimed to determine if the motion profiles would be disorienting to the astronaut rider. Testing the full motion sequence on human subjects would be difficult to perform, and if not performed on orbit might not be representative. Instead, we performed computational simulations to predict the perceptions an astronaut rider is likely to experience during the LSH motion sequence. Specifically, we simulated the “observer” model<sup>5</sup>, which has been well validated to predict human orientation perception in a wide variety of motion paradigms<sup>5-10</sup>, including altered and artificial gravity scenarios<sup>4,10-13</sup>. Using inputs of three-dimensional, inertial motion (i.e., linear acceleration and angular velocity), the observer model predicts human orientation perception. While visual cues could be incorporated<sup>6</sup>, it would require some assumptions about what the astronaut considers to be stationary. Instead, for this preliminary analysis we have simulated just the vestibular portion of the model.

In addition to the LSH motion sequence of linear acceleration, angular rotation, and linear deceleration, we simulated the rider making a head tilt. This is an important assessment because head tilts cause the disorienting vestibular cross-coupled illusion when spinning on a centrifuge AG system. We aimed to verify that the same illusion would not occur on the LSH system. We compare the actual motion (black lines in Figure 8) to that which the model predicts the rider is likely to perceive (dotted pink lines in Figure 8). When the predicted perception diverges from the actual motion, it suggests the rider may become disoriented.

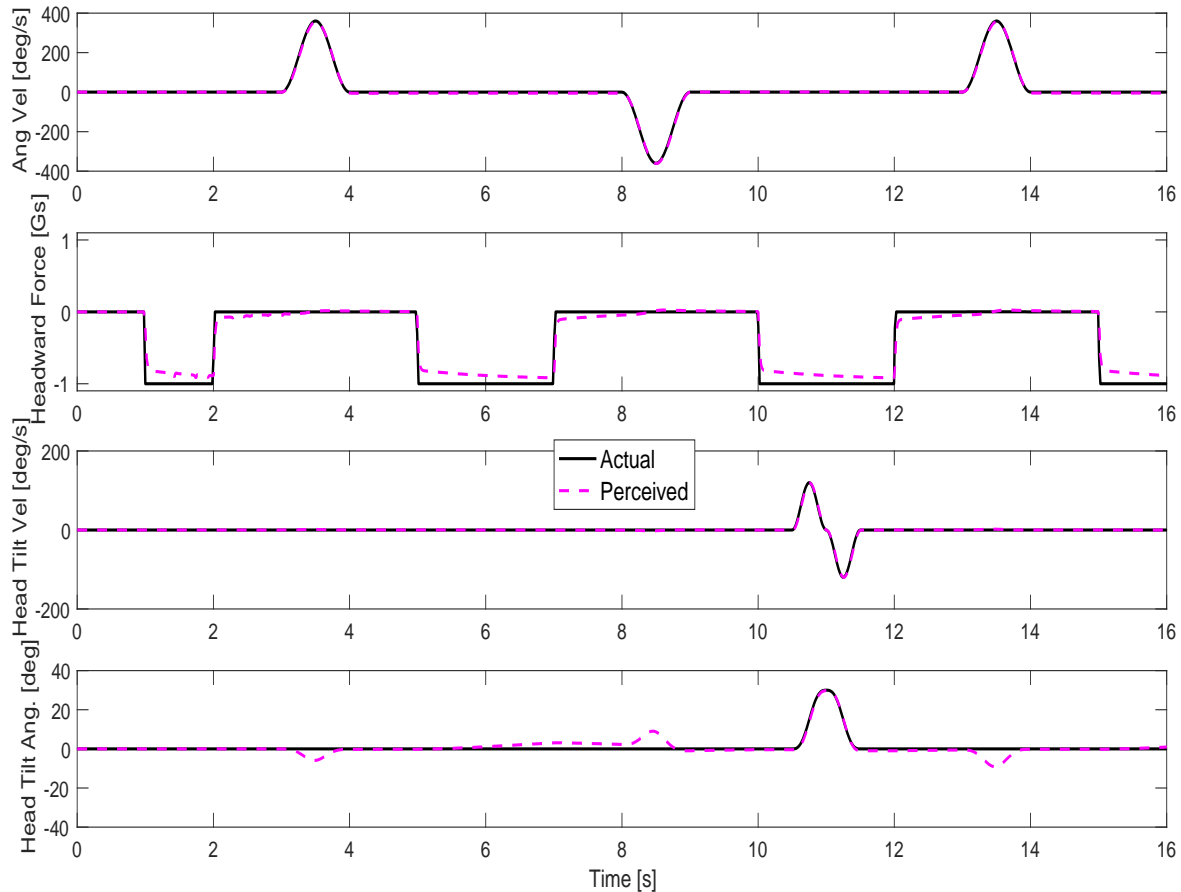


Figure 8: Observer Model Simulation of the Linear Sled Hybrid Motion Sequence - Each panel shows the actual motion in black and the model's predicted perceived motion in dotted pink. The top panel shows the 180 degree rotation and the second panel shows the headward force created by the linear acceleration and deceleration. The bottom two panels show the rider making a head tilt.

We simulated Case #1 in Table 1 of the LSH sequence in the observer model to predict the rider's orientation perception. Figure 8 shows the motion stimuli and responses at the head position. The 180° rotation and the acceleration and deceleration phases are shown in the top two panels. From 1-2s is the linear acceleration phase, 2-3s is the constant velocity transition phase, 3-4s is the 180° rotation phase, 4-5s is another constant velocity transition, and 5-6s is the deceleration phase. The 180° rotation causes this deceleration phase to also create a headward force of -1 G (i.e., a footward force), similar to standing upright on Earth. This completes one cycle of the LSH system, immediately after which the rider is accelerated back in the opposite direction (6-7s) and the sequence continues. Note that in the top panel the rotation direction alternates back and forth (as opposed to continuing in the same direction and completing a full 360 degrees across a pair of rotations). We also simulated the continuing rotation approach, but found qualitatively similar results. Furthermore, there is no asymmetry between pitch vs. roll rotation perception in this model.

As our primary finding, the model's prediction of the rider's perception (dotted pink) nearly exactly matches the actual motion (black line). Furthermore, from 10.5-11.5s, when we simulated the rider making a head tilt (bottom two panels), the perception nearly exactly tracks the actual motion for the head tilt. Finally, unlike on a short-radius centrifuge AG design, these simulations confirm that the LSH system does not cause the vestibular cross-coupled illusion when head tilts are made. This is an important benefit of the "pure" AG created on the LSH system.

In addition to simulating Case #1 in Table 1, as shown in Figure 8, we have also simulated the other cases and different rotation profiles and axes and found the results to be qualitatively similar (i.e., the model's predicted perception tracks the actual motion sequence well). This suggests the LSH motion paradigm is likely to be well perceived by an astronaut rider for a wide range of LSH motion profiles (Tables 3 and 4).

While these observer simulation results are important for demonstrating the feasibility of the LSH system in terms of avoiding rider disorientation, there are a few limitations. While the observer model is well-validated with human subject experiments, eventually it will be important to empirically validate these specific simulation predictions. It is also unclear how intermittent exposure to the LSH system (e.g., 1 hour per day) combined with predominantly microgravity exposure (e.g., 23 hours per day) will impact the astronaut rider's mechanisms for orientation perception. This is likely to remain an unknown until an AG system is tested with humans in space.

Finally, while these observer model simulations suggest astronauts are not likely to become disoriented while riding on the LSH system, the model does not predict motion sickness susceptibility. It is possible the repeated sequence of the LSH system may cause some riders to become motion sick. There is not a computational model for motion sickness of appropriate detail to simulate the LSH motion sequence. Future work should aim to assess motion sickness susceptibility with testing of humans on the ground. Conceptually, one might expect the 1 Earth G of acceleration or deceleration to not be particularly provocative since it aims to mimic the stimulation experienced when upright here on Earth. The 180 degree rotation, however might provoke motion sickness, particularly when performed quickly. (As previously noted, in order to keep the total length of the track shorter, quick rotation phases are desirable, since during the rotation phase the rider is translating at a constant linear velocity. Relatively quick rotations are also required to produce 1 Earth G of centripetal acceleration at the rider's center of mass. We have successfully performed pilot tests on humans of these repeated 180 degree rotations, with time allocated to mimic that for the interleaved linear deceleration, constant velocity, and linear acceleration phases. We aim to perform more extensive testing during Phase II to assess whether these repeated, quick 180 degree rotations will cause motion sickness or other discomfort for the rider. This validation is essential for further demonstrating the feasibility of the LSH concept.

### Subsystem Architecture:

As a preliminary step for assessing the feasibility of adding the LSH system to future long-duration crewed space exploration missions, we began a conceptual design of the LSH system. Of course, there are numerous design decisions and interactions that must be considered, as exemplified in Figure 9.

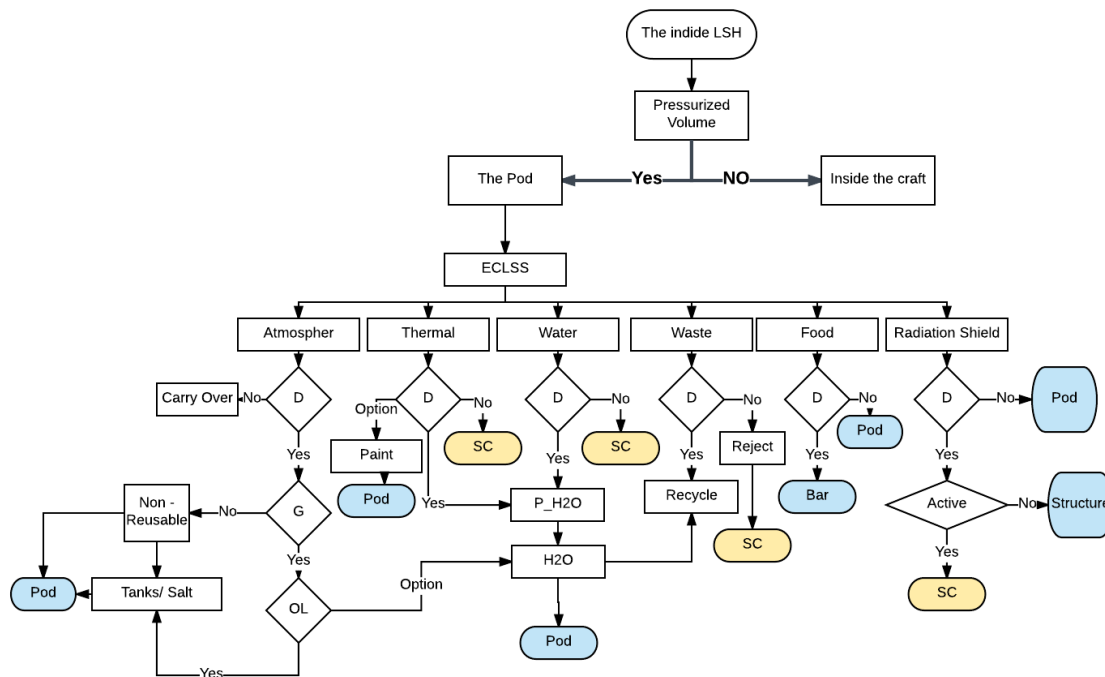


Figure 9: Pod Subsystem Design Concept Decision Diagram

### Linear Track Design

One element of the structure of the LSH system is the track on which the rider linearly translates back and forth on. In estimating the required mass of this element, there are two primary design parameters: the material (i.e., the density) and size of the track structure (i.e., the volume). The density of the material was estimated based upon the material typically used on ISS (i.e., an Aluminum Alloy is somewhat standard for spacecraft design<sup>7</sup>). As a preliminary estimate, we assumed the track consists of a single beam whose length is defined by that required for the track (the sum of that required for linear acceleration, rotation, and linear deceleration).

The high speeds created by the linear acceleration/deceleration introduce certain hazards. In the event that the deceleration phase malfunctions, a safety stop length has been built onto both ends of the track. We performed analysis to estimate the additional length of track required for this safety measure.

In summary, the translation velocities during any of the Cases in Table 1 are slow enough that the rider could be stopped in a very short distance in the event of an emergency without experiencing injury. For this analysis, we assumed a large rider (worst case) with 1.92 m height

and 85 kg weight<sup>9</sup>. The concern was that an emergency stop could cause a fracture of the rider's tibia. Therefore, we calculated the maximum allowable pressure applied to the cross-section of this bone prior to fracture<sup>10</sup>. The total energy will be conserved across the safety stop, with the kinetic energy transferring to potential energy as in Equation 2.

$$\Delta K_{\text{track}} + \Delta P_{\text{track}} = \Delta K_{\text{End}} + \Delta P_{\text{End}} \quad (2)$$

The kinetic energy transfers to physical work on to the cross-section of a tibia, applying Equations 3-4. The maximum pressure before fracturing the tibia is estimated<sup>10</sup> to be  $10^5 \text{ N/m}^2$ . The  $m$  is the mass of the person and  $v$  is the velocity at the end of the track,  $F_{\text{end}}$  is the force applied to the tibia during the safety stop, and  $\Delta h$  is the minimum distance needed to distribute the force across to avoid a fracture (Figure 1). In Equation 3,  $A$  is the cross-sectional area of two tibias (for two legs), which was assumed<sup>10</sup> to be  $0.00107 \text{ m}^2$ .

$$\frac{1}{2} * m * v^2 = -F_{\text{end}} * \Delta h \quad (3)$$

$$\Delta h = \frac{1}{2} * (2 * A) * m * v^2 / P \quad (4)$$

$$l = v_0 * t + \left(\frac{1}{2} * a * t^2\right) \quad (5)$$

$$v = v_0 + a * t \quad (6)$$

For this first order analysis, we applied a safety factor of 100x to assure the safety stopping distance was sufficient (shown in Figure 1). The “emergency stop” lengths for each Case in Table 1 were added to the nominal track lengths for each Case and are listed in Table 3. These track lengths account for the fact the 1.92 m tall rider is reoriented 180 degrees about an axis at their head (see Figure 1). This requires a minimum track length of 3.6 m (1.8m x 2 for the reorientation), even without any linear translation.

Table 5: Motion Profile and Number of Cycle per Hour

Case RMP	Case LMP	1 - Track Period (s)	Cycle per Hour
<b>A</b>	1	5.1161	704
	2	3.1161	1155
	3	1.6161	2228
<b>B</b>	1	5.2683	683
	2	3.2683	1101
	3	1.7683	2036
<b>C</b>	1	5.6743	634
	2	3.6743	980
	3	2.1743	1656
<b>D</b>	1	5.4433	661
	2	3.4433	1046
	3	1.9433	1853

Table 6: The length of the track and estimated mass and power required for various LSH configurations

Case Rotation	Case Linear	Length (m)	Mass of Track (Kg)	Average Power for Motion (Kw)	Energy per Hour of Motion (Kw-Hr)
<b>A</b>	1	43.98	5828.93	10.7034	7531.57
	2	25.36	3361.11	10.7034	12365.53
	3	6.95	921.12	4.9782	11089.36
<b>B</b>	1	45.58	6040.99	10.6845	7301.06
	2	25.85	3426.05	10.6845	11768.87
	3	7.32	970.16	3.6009	7330.91
<b>C</b>	1	49.46	6555.23	7.7205	4898.19
	2	29.84	3954.87	7.7205	7564.38
	3	8.32	1102.70	2.1185	3507.61
<b>D</b>	1	47.29	6267.62	9.1135	6027.34
	2	27.58	3655.34	9.1135	9528.24
	3	7.75	1027.15	2.7460	5087.02

Table 6 shows that the track length can vary substantially depending upon the combination of G-level during acceleration/deceleration, duration of each phase (Cases 1-3 from Table 3) and the profile of the rotation phase (Cases A-D from Table 4). Some track lengths were fairly long (e.g., that for Case #1 of the linear motion in which there was 1 second for each of the linear

acceleration, two transitions, and linear deceleration phases). However, we emphasize that in other designs, the track length could be very modest. For example, Case #3 of the linear motion, in which there were no transitions and only 0.25 seconds for each linear acceleration/deceleration, only required around 7 m of track length. This included the 3.8 m of length required for reorienting the rider 180 degrees about their head, as well as the emergency stop length. Table 5 includes the total time required per 1 time travel of track and also number of cycles that can be completed in 1 hour. (We further note that Table 5 and 6 does not include linear motion Case #4 which was designed to create Mars gravity during the linear acceleration/deceleration phases, as compared to Cases #1-3 which created 1 Earth G. Of course, the reduced G-level yields an even shorter track length.)

Based upon these track lengths, we estimated the required mass of the track structure; however we emphasize these are preliminary and should be considered only at a conceptual level. A more detailed structural design is required to more precisely estimate the required mass of the structure. The mass of the track was estimated by assuming that the material used was a single cylindrical beam of aluminum (defining the density,  $\rho$ , of the structure) and calculating the volume based upon the length (L) of the track and an assumed beam diameter of 0.25 m (radius,  $r=0.125$ m).

$$m_{track} = \rho * (\pi * r^2 * L_{track}) \quad (7)$$

The mass required for the structure of the beam is shown in Table 6 for each of the various configurations. Again, we reiterate these are conceptual estimates that require refinement.

Next we aimed to provide a preliminary, theoretical estimate of the power required for producing the translation (acceleration and deceleration) and rotation of the LSH system. As detailed in the next session, this was dependent upon the mass that needed to be moved, which consisted of the rider and the pressurized pod capsule in which they were housed. We calculated the power required as a function of time during the LSH motion sequence. The total energy required to power the system for one hour is shown in Table 3 for each configuration, and calculated using the equations below. The power required for the rotation phase ( $P_R$ ) was determined using equation 8, where M is the combined mass of the pressurized pod, rider, and counterbalance (details below), L is the length from the center of the rider's head to their feet (Figure 3),  $\alpha$  is the instantaneous angular acceleration, and  $\omega$  is the instantaneous angular velocity during the rotation phase. We assumed there to be minimal rotational friction.

$$P_R = \left(\frac{1}{12}\right) * M * (2L)^2 * \alpha * \omega \quad (8)$$

$$[Kw] = 0.001 * [Kg * m^2 * rad/s * rad/s^2]$$

The power required for the linear motions ( $P_L$ ) was estimated using equation 9, where a is the linear acceleration/deceleration magnitude and V is the instantaneous linear velocity. We also assume there to be minimal kinetic friction during linear motion.

$$P_L = M * a * V \quad (9)$$

**Design of a Pressurized Pod:**

We had initially conceptualized that the rider and the entire track on which the linear and rotational motion of the LSH motion sequence occurs would be housed within a large pressurized module. This has the advantage that the entire system would be in a pressurized module (i.e., for servicing the LSH mechanical systems, etc.). However, particularly for the longer track length configurations (e.g., Case #1 in Table 3), this would require a fairly large additional pressurized volume.

As an alternative, we have proposed that the rider be enclosed in a fairly small pressurized pod that then experiences the LSH motion profile (Figure 10). The approach is similar to the “Single Person Spacecraft” concept proposed by NASA engineers at Huntsville<sup>26</sup>, except here the pressurized pod is not maneuverable beyond the LSH motion profile. The “pod” concept has the tremendous advantage of reducing the required pressurized volume to that just large enough to house a single rider comfortably (e.g., similar to a phone booth or small shower). However, it does present some additional engineering and logistical challenges. As the pressurized pod translates on the LSH track, it would need to be disconnected and sealed off from the primary pressurized vehicle/habitat during operation. If the operating pressures in the pod and primary habitat are the same, it would not necessarily require an airlock, but would require a hatch that could be opened for entering and exiting the pod from the habitat and then closed and sealed during operation of the LSH system. We tentatively assume that these logistical and engineering challenges can be overcome, and continue our conceptual design with the pressurized pod concept.

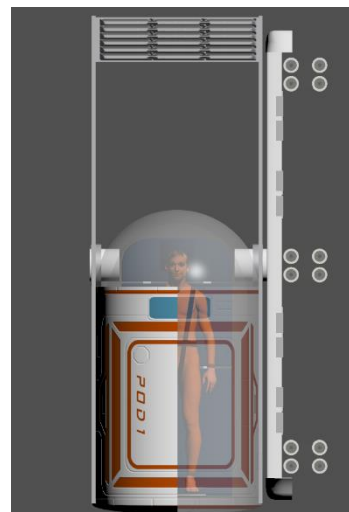
We briefly note, that an even more “minimalist” approach could be taken in which the astronaut is just in a pressurized spacesuit, exterior to the habitat, and the LSH system provides no pressurization. The limitation to this is that it would require an airlock and pre-breathe time to acclimate to the reduced pressure of the spacesuit for each use, which seems unreasonable for a system that is used daily.

**Environmental Control and Life Support Systems (ECLSS)**

One of the challenges of the pressurized pod concept, is that the pod itself will need to provide Environmental Control and Life Support System (ECLSS) functionality during operation when a rider is inside. Estimates for the ECLSS requirements are shown in Table 7, based upon an 85 kg male (NASA Life Support Baseline Values and Assumptions Document (BVAD), 2015)<sup>9</sup>.

Table 7: ECLSS Input and Output for a Crew Member (Cm)

In Put	Kg/Cm-2.5 Hr
O2	0.085
Food	0.157
Water	0.105
<b>Total</b>	<b>0.347</b>
Out Put	Kg/Cm-2.5 Hr
CO2	0.108



Solid Waste	0.067
Water Waste	0.38
<b>Total</b>	<b>0.555</b>

Figure 10: Pod and the Counterweight

### Habitable Volume of Pod

As a preliminary estimate, we quantified the habitable volume of the pressurized pod to be equal to that of the sleeping quarters in the ISS<sup>11-13</sup>. As we desire for the center of rotation of the pod to be aligned with the rider’s eye/ear location, there is an adjustable footplate to maintain positioning for astronauts of different heights. The pod also has a counter weight arm to help with rotation. The approximate dimensions of the pod concept are shown in Figure 11.

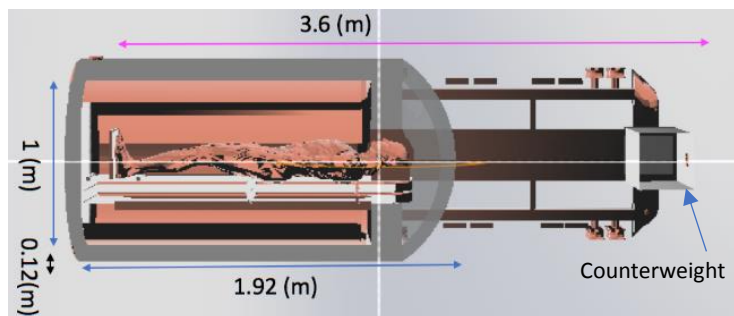


Figure 11: Pod Dimension

Future analysis will aim to assess the structural integrity of the pod and the required thickness of the walls given the pressures applied to its interior (Figure 12). For now, we assume the structure of the pressurized pod to be aluminum, allow with a thickness of 0.12m, based upon that used for the thickness of the pressurized hull of the ISS<sup>12</sup>.

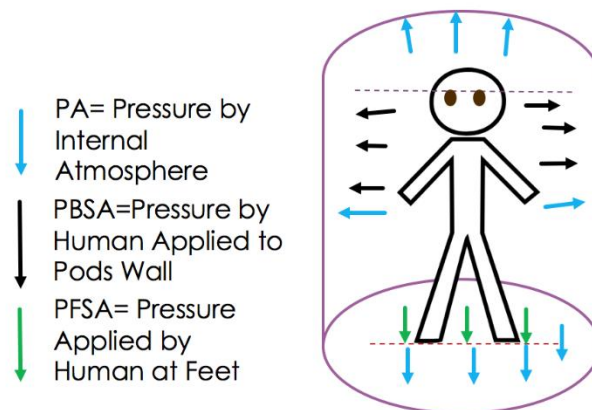


Figure 12: Pressures Applied to the Wall of Pod

## Atmospheric Conditions and Revitalization

As mentioned above, it is beneficial for the atmosphere in the pod to match that of the existing vehicle/habitat. Particularly, because we envision the LSH system to be used intermittently, on a daily (or nearly daily) basis, it is essential that it can be easily entered/exited without an airlock or risk of decompression sickness. Thus, we assumed the pressurized pod to have an atmosphere matching that typical for an exploration vehicle (10.2 Psia, Table 4-1 and 4-2 in BVAD 2015)<sup>9</sup>.

When not in operation, the pressurized pod would be open to the primary habitat and with sufficient fans/ventilation, the atmosphere in the pod would equilibrate to that in the habitat. This would allow for the LSH pod's atmosphere to be maintained by the existing atmosphere revitalization system in the habitat. However, during operation, the pressurized pod would need to be sealed off from the primary vehicle/habitat and thus an allowable atmosphere must be maintained in isolation. For this analysis, we assumed the upper limit of operation for the pod being sealed would be 2.5 hours. Just prior to beginning operation, the atmosphere in the pod would be assumed to be equilibrated to that in the habitat, which was again assumed to be that for an exploration vehicle shown in Table 8 (BVAD, Table 4-1 and 4-2)<sup>9</sup>:

Table 8: Gas Composition inside Pod at Start

Gas	%Concentration	Pressure (Pisa)
O <sub>2</sub>	26.5	2.78
CO <sub>2</sub>	0.76	0.078
N <sub>2</sub>	72.74	7.42
Total	100	10.2

During sealed operation of the LSH system, the rider would consume O<sub>2</sub> and produce CO<sub>2</sub> within the pressurized pod (Figure 13). We assessed how much O<sub>2</sub> consumption and CO<sub>2</sub> production would occur by the end of the upper limit of 2.5 hours of operation. If the fractional O<sub>2</sub> level became too low or the CO<sub>2</sub> too high, we could add appropriate atmosphere revitalization systems to the pod.

Based upon the rough dimensions in Figure 11, the interior volume of the pod is 1.56 m<sup>3</sup>. We estimate the volume of a typical crewmember<sup>12</sup> to occupy approximately 0.075 m<sup>3</sup>, leaving 1.485 m<sup>3</sup> of volume for the atmosphere, corresponding to 1.78 kg of air within the pod. Given the atmospheric partial pressures above, this corresponds to 0.47kg of O<sub>2</sub> at the beginning of the pod being sealed. Using standard values, approximately 0.085kg of O<sub>2</sub> will be consumed in 2.5 hours, yielding a final composition of O<sub>2</sub> of 21.6%. This is sufficiently above the level for clinical hypoxia (~16% O<sub>2</sub>). Therefore, based upon initial analyses, it is reasonable to operate the sealed pod without oxygen (re)generation.

Next, we consider CO<sub>2</sub> production during the 2.5 hour period. Assuming the temperature is 20 C, air density is 1.2 kg/m<sup>3</sup>, and humidity is 50%, the maximum CO<sub>2</sub> production per hour by a single crew member is 0.29 psia (NASA HIDH), corresponding to an added 0.108kg of CO<sub>2</sub>. With the initial mass of CO<sub>2</sub> of 0.0135kg, after 2.5 hours the CO<sub>2</sub> mass will increase up to 0.1215kg, corresponding to a composition of 6.82% CO<sub>2</sub>. This yields a partial pressure (pp) of 0.68 Psia, which is well above that which is allowable (0.29 Psia) to avoid early stages of CO<sub>2</sub> poisoning (e.g., headaches).

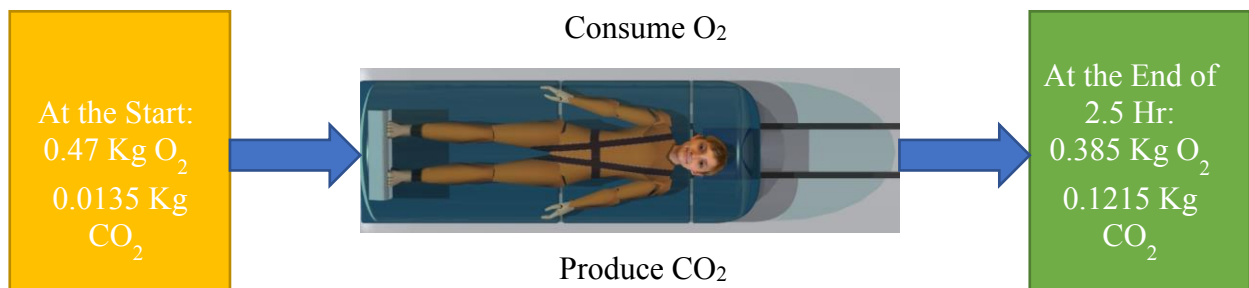


Figure 13: Human O<sub>2</sub> and CO<sub>2</sub> Balance

Therefore, it is necessary to include onboard CO<sub>2</sub> capture within the pod during operation. The selection of a CO<sub>2</sub> scrubbing system within the pod depends upon the mission architecture and technologies that will become available in the future, but below are a few options that are currently available<sup>15</sup>:

- CO<sub>2</sub> Regenerable System
  - **Electrochemical Depolarization Concentration (EDC)**
    - Uses fuel-cell type reaction to concentrate CO<sub>2</sub> at the anode
    - $\text{CO}_2 + 1/2\text{O}_2 + \text{H}_2 \rightarrow \text{CO}_2 + \text{H}_2\text{O} + \text{electricity} + \text{heat}$
    - CO<sub>2</sub> and H<sub>2</sub> are collected at anode and directed to CO<sub>2</sub> recycling system
    - 11 kg; 0.02 m<sup>3</sup>; 60 W (all per kg-day of CO<sub>2</sub> removal); does not include reactants for power output – TRL 6
- CO<sub>2</sub> Non-Regenerable
  - **LiOH Mass Estimating Factor Space Shuttle**
    - LiOH system uses a 7 Kg cartridge, good for 4 crew-days = 1.75 kg/crew/day
    - 0.003 m<sup>3</sup>/canister - TRL 9

Lastly, we note that the CO<sub>2</sub> capture system could be non-regenerable during LSH system operation, but regenerable after operation by leveraging a hardware on the existing vehicle/habitat for the function of regeneration. This has the advantage that the regenerable hardware and associated mass would not have to be onboard the pod. Any added mass to the pressurized pod has to be translated and rotated through the LSH motion sequence, requiring added power.

### Additional ECLSS functions

As the pressurized pod will regularly be connected with the existing habitat/vehicle, we assume that trace contamination will be filtered through existing systems in the main cabin.

In the maximum of 2.5 hours, we do not anticipate a need for a waste management system during LSH operation.

A small amount of water (e.g., water bottle) and food (e.g. granola bar) will be sufficient for the 2.5 hours of operation.

Thermal control of the heat generated by the crew member riding in the pod requires further study. However, we note that since the LSH motion sequence generates linear acceleration, there will be free convection in the cabin of the pod. Therefore, a water loop jacket, heat emission, and small fan should be sufficient for this thermal control.

### Radiation Shield

We have assumed that nominally each crew member would ride in the LSH system 1 hour per day, with an upper limit of 2.5 hours. Even at 2.5 hours, this would yield only ~10% of each crew member's day (24 hours) in the LSH system. Thus it may not be as critical to add substantial radiation shielding to the LSH pressurized pod, as compared to the primary habitat. Furthermore, adding radiation shielding increases the mass of the pod, which increases the power required for translation and rotation of the LSH system. For example, including 20 g/cm<sup>2</sup> of Polyethylene radiation shielding dramatically increases the mass of the pod system (Figure 14), even more so with the NASA recommended shielding for the ISS<sup>17-18</sup>.

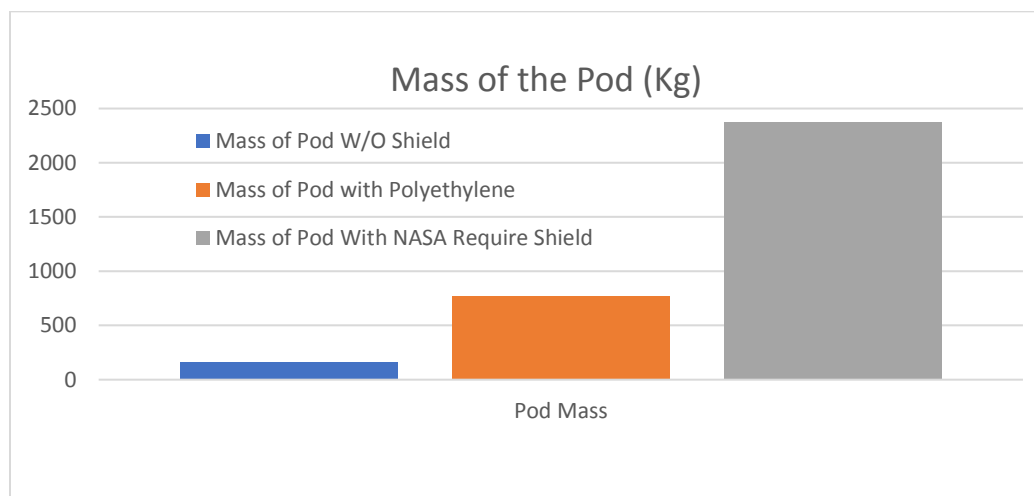


Figure 14: Pod Mass Trend by Adding Radiation Shield

Thus, it may make more sense to include minimal radiation protection in the LSH system and instead focus shielding on the primary vehicle. This probabilistic analysis to radiation risk is only appropriate for nominal radiation levels, primarily from galactic cosmic rays. In the event of a solar particle event temporarily elevating radiation levels, we suggest the astronauts would just not use the LSH system until the event passes. This seems like an appropriate tradeoff between concept of operations and engineering feasibility.

Table 5 shows a summary of estimated masses required for the pressurized pod portion of the LSH system. There are also relatively small power requirements for outfitting the interior of the pod (e.g., lighting, fans, the minimal ECLSS and thermal systems described above). Future study should further refine these conceptual estimates. With a 2.5% margin, the mass of the pod without any added radiation shielding was estimated to be 158 kg and the power for internal system was estimated to be 8.5 Kw.

Table 9: Mass and Power of Pod

Name	Material	Length (m)	Width (m)	Height (m)	Pod Mass (Kg)	Pod Power (Kw)
Pod Interior + human	TBD	1	0.38	1.98	88	0.5
Radiation shield	Polyethylene	1.12	0.06	2.1	Depends	N/A
Pressurized Housing	MMOD+ Kapton + Air+Al 2319	1.1444	0.0122	2.0044	34	N/A
Window	Glass	0.5	0.05	0.5	29.125	N/A
ECLSS	N/A	1.04	0.56	1	0.5	3
Thermal	Water Aluminum	TBD	0.02	TBD	3	5

### Actuation Subsystem

The LSH system requires a subsystem which is responsible for providing the linear translation and angular rotation of the motion sequence. At this point, we have only considered various approaches for how this might be performed and conceptually assessed the benefits and drawbacks of each approach.

One approach is to use a linear motor(s) to provide the translation and a second rotational motor to actuate the 180-degree rotation. In this approach, the rotational motor, pressurized pod, and non-rotating platform would all need to be translated back and forth. This would add to the total mass that needs to be linearly accelerated and decelerated, thus increasing the power draw and capability requirements of the linear actuators. It also adds additional parts and motors to the system that may fail and would require maintenance and potentially spares. One substantial advantage is that the system could easily be programmed to allow for different G-levels and durations of each phase. For example, if the linear track was desired to be long enough for 1 second acceleration/deceleration phases (i.e., Cases #1-2 in Table 3), it could also be operated using only 0.25 seconds for these phases (i.e., Case #3 in Table 3). In this case, only a shorter portion of the mechanical track length would be utilized and the rotation would be programmed to occur earlier in the sequence. Such an approach would be highly beneficial for the initial on-orbit system to allow for testing out different configurations.

Another approach is to use just one set of linear motors and actuate the rotation using a curved guide track. As the pressurized cab translates down the guide path, the pin in the curved guide path forces the 180 degree rotation with the specific profile. We have developed a functional, 1/20<sup>th</sup> scale prototype of such a system that we demonstrated at the 2017 NIAC meeting <sup>19</sup>(Figure 15).



Figure 15: 1/20th scale model of the guide track actuation approach

This approach has the potential advantages of requiring less mass, power, and maintenance than having a second motor for rotation. Though we note there would be added friction from the pin being deflected along the guide path are compared to pure linear translation. It also may be more dependable, since the 180 degree rotation is forced to occur at the same time and with the same profile during each sequence. One potential disadvantage of this approach is that the rotation profile, sequence timing, and acceleration/deceleration durations and G-levels are fully defined by the curved guide path and thus cannot be altered simply by reprogramming. Furthermore, with a single guide path, it requires the rotation direction to alternate between the motion sequence from left to right and that from right to left. This may be less desirable if one rotation direction is less tolerable to the rider (e.g., pitch backward vs. pitch forward).

### Cost Estimate for the LSH Concept:

We aimed to produce a preliminary cost estimate of the LSH system to assess feasibility. However this was a challenging task due to the lack of detailed designs for many of the subsystems. Future work will aim to refine the concept and help better assess the cost-benefit of the system. Here, we developed a preliminary cost estimate via applying the well-established Johnson Space Center Advanced Mission Cost Model (AMCM). The AMCM provides a top-down cost estimate for a mission (in \$million 1999 dollars<sup>20</sup>) based primarily upon the mass of the system.

$$COST = \alpha * Q^{\beta} * M^{\Xi} * \delta^S * \varepsilon^{\left(\frac{1}{IOC-1900}\right)} * B^{\varphi} * \gamma^D$$

The Greek letter constants are:  $\alpha = 5.65 \times 10^{-4}$ ,  $\beta = 0.5941$ ,  $\Xi = 0.6604$ ,  $\delta = 80.599$ ,  $\varepsilon = 3.8085 \times 10^{-55}$ ,  $\varphi = -0.3553$ ,  $\gamma = 1.5691$ . In the equation above: Q is the quantity of the product/vehicle to be produced. M is the total dry mass of the system in pounds, S is the specification (value that designates the type of mission to be flown, in our case we used a human habitat, such that S=2.13). IOC is defined as Initial Operational Capacity (i.e., the year in which the system would first be in operation). B is the Block Number, which corresponds the level of design inheritance (as the LSH concept is a new idea, B=1). D is the level of difficulty, which was

assumed to be moderate for the LSH concept. Table 10 shows a preliminary estimate of the costs of the LSH system, though we emphasize these values require refinement. Notably, the mass of the linear track structure is likely to be excessive, and thus this estimated total cost is too high<sup>20-23</sup>.

Table 10: Cost Estimate Model- Cost Calculated in Million Dollars

Parameters	Pod with Counter Mass	Track Min Length	Track Max Length
Q	1	1	1
M	316	3510.61	12368.53
S	2.13	2.13	2.13
IOC	2030	2030	2030
B	1	1	1
D	0	0	0
<b>Total Cost M \$</b>	300.28	1472.68	3383.01

### Risk Assessment and Failure Mode and Effects Analysis

Even at this early stage of development of the LSH system concept, it is important to begin to identify risks and their associated impact. We performed a risk assessment analysis, identifying the relevant risks associated with the LSH system. Some of the risk areas are shown in Table 11 and Figure 15 shows where those risks might fit in terms of likelihood (the probability of the risk occurring) and consequence (how serious is the impact if the risk does occur). More information is provided in the Appendix on the Risk Definition and Risk Data Base<sup>24</sup>.

Table 11: Identified Risk and Mitigation

Risk #	Risk Title	Class	Risk
1	Transit Gravity	Mitigate	Medium
2	Vibration	Mitigate	Medium
3	Development	Watch	Medium
4	Assembly	Watch	High
5	Stop at the End	Watch	Medium
6	ECLSS	Research	Low
7	Radiation - Communication	Watch	High
8	Fire	Mitigate	Low
9	Connection to Airlock	Mitigate	Medium
10	Power Failure	Watch	Medium
11	Actuator and Railing	Research	High

Likelihood	5					
	4				7,11	
	3				2,9,10	4
	2			6	1	3,5
	1			8		
		1	2	3	4	5
		Consequence				

Figure 15: Risk Matrix

In addition to the Risk Analysis, a Failure Mode and Effects Analysis (FMEA) was conducted<sup>25</sup>. Some of these considerations are shown in Table 12. As the system is further developed, this analysis will be refined (the acronyms in Table 12 are defined in the acronym list).

Table 12: FMEA Analysis for Turbolift NIAC Phase I

Key Process Step or Input	Potential Failure Mode	Potential Failure Effects	SEV	Potential Causes	OC	Current Controls	DET	RPN
What is the Process Step or Input?	In what ways can the Process Step or Input fail?	What is the impact on the Key Output Variables once it fails (customer or internal requirements)?	How Severe is the effect to the customer?	What causes the Key Input to go wrong?	How often does cause or FM occur?	What are the existing controls and procedures that prevent either the Cause or the Failure Mode?	How well can you detect the Cause or the Failure Mode?	
LSH								
Material and Component Integrity	Component Break	Assembly and Operation Failure	4	Transient Gravity	2	Flight Ready Equipment	10	80
Material and Component Integrity	Component Break	Assembly and Operations Failure	4	Vibration	3	Flight Ready Equipment	10	120
Material and Component Integrity	Loss of Launch	Assembly and Operations Failure	5	Loss of Craft	2	Flight Ready Equipment	10	100
Assembly and Operation	Loss of Human and Technology	Assembly and Operations Failure	5	Human Factor Failure	3	Training in Advance	10	150
Functional Failure	Loss of Human and Technology	Safety Failure	2	Design Failure - Stop at the End	5	Built in safety factor	10	100
Keeping Crew Alive	Loss of resources	Redundancy	3	ECLSS	2	Redundancy	10	60
Crew Accommodation	Extended time in the LSH	Redundancy	4	Radiation Effect on Communication	4	Watch Dog and Rest	10	160
Keeping Crew Alive	Cluster and Atmospheric Control	Operations Failure	3	Electric Fire	1	O2 Concentration <30%	10	30
Assembly and Operation	Extended time in the LSH	Assembly and Operations Failure	4	Connection to Airlock	3	Redundancy	10	120
Keeping Crew Alive	Extended time in the LSH	Assembly and Operations Failure	4	Power Loss	3	Alert System in The Craft	10	120
Keeping Crew Alive	Extended time in the LSH	Redundancy	4	Railing	4	Alert System in The Craft	10	160

## Summary of Feasibility

In our analysis and preliminary conceptual design of the LSH system, we did not uncover any reason why the system would be infeasible for use in future long-duration space exploration missions. Conceptually, it seems quite likely to be beneficial in reducing or fully mitigating the physiological deconditioning that astronauts otherwise experience during long-duration space exploration. This is highly critical to ensure the astronauts' well-being and their ability to perform mission critical tasks (e.g., extravehicular exploration on the surface of Mars). We suggest such a system would be enabling for crewed space missions with extended durations (e.g., > 6 months).

We performed analyses exploring different motion sequences (i.e., various phase durations, G-levels, and rotation profiles), weighing the advantages and disadvantages of each. At this point, it is unclear which optimizes the tradeoff in the benefit to the astronauts while reducing cost and improving tolerability, but our analysis outlines the trade space.

We performed computational simulations using the well-validated “observer” model to demonstrate that the LSH motion sequence is unlikely to be disorientating to the rider. We verified that the LSH will not create any vestibular Coriolis cross-coupled illusion, which is typically disorienting and leads to motion sickness on a short-radius centrifuge. Furthermore, the “pure” AG during the linear acceleration and deceleration phases of the LSH system will not create any Coriolis forces of gravity gradients that again are typical of a short-radius centrifuge. Future work will need to validate our pilot testing to show the motion sequence is tolerable in terms of motion sickness and general comfort. Our preliminary analysis suggests that the LSH motions are tolerable and that the motion sequence can be modified (in terms of G-level, durations, and rotation profile) to optimize comfort to the rider.

Preliminary estimates of the mass, power, volume, and cost of the LSH system were made for various configurations. In this effort, we proposed using a small pressurized pod to house the astronaut rider during LSH operation. This approach reduced the required pressurized volume, but may introduce some logistical and engineering challenges, as we have identified. The analyses suggest the system to be feasible, though future analysis should be performed to refine these estimates and conceptual designs. Finally, we considered some risks to the LSH system.

Table 13: Total Mass, Power, and Cost Estimates of the LSH (Pod, Counterweight and Track)

Case	Mass (Kg)	Power/Energy (Kw-Hr)	Cost M\$
Min	6871.2276	3510.61	1772.96
Max	1237.1248	12368.53	3393.72

## Integrating into Future Mission Concepts

The LSH system is likely to be beneficial to any future crewed long-duration space exploration mission concept. During missions of at least 6 months of microgravity exposure, astronauts experience physiological deconditioning that can be incapacitating. This impacts not only their health and well-being, but their ability to perform critical tasks. In order to enable long-duration, exploration-class crewed missions, it is essential that astronauts are able to physically function at a high level. For example, during a crewed mission to the surface of Mars,

astronauts will need to be excellent physical health to perform tasks such as extravehicular activities (EVAs). With the current piecemeal approach of exercise, diet, and pharmaceutical countermeasures, it is uncertain whether they will be able to perform such tasks at a high level, at least immediately after landing. The LSH replicates the loading of gravity here on Earth, presumably mitigating deconditioning and allowing for improved astronaut performance.

The LSH system is applicable to *any* crewed long-duration mission, regardless of destination. Certainly, we envision direct applications to crewed Mars exploration missions due to the required 1-3 year duration with current propulsion technologies (at least 1 year of cumulative microgravity exposure), whether that mission includes a surface stay or is just orbital. It is also beneficial for other deep space destinations, such as cis-lunar space, if the mission is of sufficiently long duration. In the more distance future, human exploration beyond Mars, to destinations such as orbiting Europa, is almost certainly infeasible without a gravity loading countermeasure such as the LSH system.

Notably, the system can easily be integrated into various existing spacecraft or vehicle designs. The LSH system is situated on the exterior of an existing spacecraft and does not occupy existing habitable volume. We have assumed some of the ELCSS functionality of the LSH system would be provided by the existing spacecraft, though this design could easily be modified. Therefore, the LSH system concept is modular and can easily be added to various spacecraft designs depending upon the mission and destination.

### **Integrating into Planetary Missions**

For the majority of our analysis, we focused on integrating the LSH system into a microgravity habitat and aimed to create 1 Earth G of loading. However, as briefly noted early (Case #4 in Table 3) during transit prior to landing on the surface of Mars, it may be beneficial to replicate the 0.38 G of Mars in preparation for that environment. In particular, the sensorimotor/neurovestibular system that coordinates balance, locomotion, orientation perception, and other functions, may benefit from prior 0.38 G exposure. If the astronauts intermittently experience 0.38 G with the LSH system on transit to Mars they are likely to be better prepared to physically perform immediately following their landing on Mars.

Beyond this physiological benefit, having the G-level during the acceleration and deceleration phases be only 0.38 G offers a huge advantage in reducing the required track length. With lower G-levels, the acceleration and deceleration phases require much less track length, but also the peak linear translation velocity is much lower, requiring less track length for the same duration of rotation and any transition phases. For example, comparing Case #4 (0.38 G) vs. Case #2 (1 G, but otherwise the same duration for each phase), the track length reduces by approximately a factor of 3 (e.g., from about 30 m for 1 G to about 10 m for 0.38 G, depending upon the rotation profile). On the other hand, loading at only 0.38 G may be insufficient to be protective for bone loss, muscle weakening, cardiovascular deconditioning and visual changes. Also we note that it becomes a greater burden to create a 180 degree rotation profile that aims to create only 0.38 G of centripetal acceleration at the rider's center of mass. To do this would require a much slower angular velocity, causing the rotation phase to become quite long. This causes the majority of the sequence duration to be dominant by the rotation phase and not the linear acceleration/deceleration phases. Instead we suggest a rotation profile that yields more than 0.38 G at the rider's center of

mass. This would elevate the loading that needs to be supported by the rider's legs and feet (potentially improving the mitigation of musculoskeletal deconditioning). However, there would be no gravito-inertial stimulation to the vestibular system in the rider's head, as this is the location of the center of rotation.

Another important consideration for the potential use of the LSH system is how it might benefit missions that involve an extended stay on a planetary surface. It is currently unknown whether an extended stay in 0.38 G on Mars or 0.16 G on the moon will be sufficient to prevent astronaut physiological deconditioning. Until it has been shown that these G-levels are sufficient, it may be beneficial to use the LSH system on the surface of these planetary bodies. In this scenario, the combination of LSH accelerations and the planetary gravity would yield net gravito-inertial forces that would not be aligned with the rider's longitudinal body axis, even during the pure acceleration and deceleration phases. However, the ability to create a full 1 Earth G through the LSH motion sequence may be essential for mitigating potential astronaut physiological deconditioning from long-duration exposure to reduced gravity during planetary stays.

## Future Work

Demonstrating the efficacy of the LSH system in reducing astronaut physiological deconditioning is challenging without such a system on orbit to test with astronauts. Ground-based analogs, such as head-down tilt bed rest for musculoskeletal and cardiovascular deconditioning, could be used for a preliminary demonstration. In such testing, one group of subjects would undergo extended bed rest while another group would undergo the same bed rest, but with a daily exposure to the LSH system on the ground. We hypothesize the daily exposure to the loading sequence of the LSH system would mitigate the physiological deconditioning of the pure bed rest group. This testing requires a full-size, human-rated LSH system constructed on the ground, as well as performing bed rest testing, which typically requires specialized facilities. Furthermore, bed rest is not an appropriate spaceflight analog for several physiological systems, and eventually these studies would need to be validated on orbit. Nonetheless, it is reasonable to be confident that replicating the gravity loading here on Earth through the LSH system will indeed be beneficial in mitigating astronaut deconditioning.

Future work should aim to better quantify the rider's tolerability of the LSH motion sequence. Particularly, repeatedly performing the rotation phase at high speeds may provoke motion sickness or be uncomfortable due to large tangential accelerations. Performing the 180 degree rotation more slowly (e.g., in 3 or 4 seconds) would presumably be more tolerable. However, a longer duration rotation phase requires a much longer linear sled track length, since during that rotation the rider is still translating at peak linear velocity. Also a slower rotation would not produce a full 1 Earth G of centripetal acceleration at the rider's center of mass, which might be less beneficial. In the future, we aim to perform ground-based human testing to assess the feasibility/tolerability of the repeated 180 degree rotations of the LSH motion sequence, when performed over the shorter durations shown in Figure 6 (e.g., 1.4 seconds).

Another important area of future work is to better understand the physical interactions between the LSH system and the primary habitat/vehicle. The repeated motion sequence will impart forces, torques, and vibrations on the habitat. In the future, we aim to perform conceptual design analysis and build a motorized scale model of the system that can be used to quantify these

physical interactions. Specifically, we envision performing testing during parabolic flight with an instrumented physical model to quantify the impact. This will be important for demonstrating the feasibility of the linear sled system in a microgravity environment.

### Publications

1. Vincent, G., Gruber, J., Reed, B., Newman, M.C., and Clark, T.K., “Observer Model Analysis of Orientation Perception during Artificial Gravity Stimulation via Centrifugation versus Linear Sled” (abstract and presentation) 32<sup>nd</sup> American Society for Gravitational and Space Research Conference, Cleveland, OH, 26-29 Oct, 2016.
2. Gruber, J.An., Seyedmadani, K., Vincent, G., Reed, B., Gruber, J.Al., and Clark, T.K. “A Novel Linear Sled “Hybrid” Artificial Gravity Countermeasure for Microgravity-Induced Physiological Deconditioning” (abstract and poster) NASA Human Research Program Investigator’s Workshop, Galveston, TX, 23-26 Jan, 2017.
3. Clark, T.K., Seyedmadani, K., and Gruber J. “Turbolift – A Linear Sled Hybrid Approach to Artificial Gravity” (presentation and poster) NASA Innovative and Advanced Concepts Symposium, Denver, CO, 25-27 Sept, 2017.
4. Seyedmadani, K., Vincent, G., Gruber, J.An., Gruber, J.Al., Cooper, V., and Clark, T.K. “The Linear Sled “Hybrid” Approach to Artificial Gravity as a Countermeasure for Crewed Long-Duration Space Exploration Missions” AIAA Space Conference, Orlando, FL, 12-14 Sep, 2017.
5. Seyedmadani, K., Gruber, J.A., Vincent, G., and Clark, T.K. “Linear Sled-Hybrid Artificial Gravity as a Comprehensive Countermeasure for Astronaut Physiological Deconditioning” (abstract and poster) NASA Human Research Program Investigator’s Workshop, Galveston, TX, 22-25, Jan, 2018.
6. Seyedmadani, K., Gruber, J.A., Clark, T.K. “The Linear Sled “Hybrid” Approach for Artificial Gravity as a Countermeasure for Crewed Deep Space Gateway Missions” (abstract and presentation, accepted and awaiting conference) Deep Space Gateway Science Workshop, Denver, CO, 27 Feb-1 Mar, 2018.
7. Vincent, G., Gruber, J., Newman, M.C., Clark, T.K. “Analysis of Artificial Gravity Paradigms using a Mathematical Model of Spatial Orientation” (submitted and under peer-review) Aerospace Medicine and Human Performance 2018.

### Outreach and Public Engagement

Interview on Colorado Public Radio in conjunction with the NIAC Symposium in Denver, CO.

### Acknowledgements

We acknowledge Dr. Gilles Clement (NASA) for his feedback on AG, Prof. James Nability (University of Colorado-Aerospace) for his help on ECLSS conceptual design, Daniel Case (University of Colorado-Aerospace) for his help on radiation shielding design, Grant Vincent (University of Colorado-Aerospace) for performing observer model simulations, members of the Bioastronautics Laboratory (Jordan Dixon, Kathrine Bretl, Sage Sherman, Thomas (T.R.) Mitchell, Sebastian Metcalf, and Carson Brumley) for assistance operating the Human Eccentric Rotator Device during pilot testing, the helpful feedback of Dr. Bryan Reed, the video expertise of Perry Papadopoulos, and Vaughn Cooper for engineering support.

## List of Acronyms

AG	Artificial Gravity
AMCM	Advanced Mission Cost Model
CM	Center of Mass
Cm	Crew Member
CO <sub>2</sub>	Carbon Dioxide Gas
DET	Detectability
ECLSS	Environmental Control and Life Support Systems
FMEA	Failure Mode and Effect Analysis
FT	At Feet
G	Gravity
HIDH	Human Integration Design Handbook
Hr	Per Hour
IOC	Initial Operational Capacity
ISS	International Space Station
LMP	Linear Motion Profile
LSH	Linear Sled Hybrid
N.A	Not Applicable
N <sub>2</sub>	Nitrogen Gas
NASA	National Aeronautics and Space Administration
NIAC	NASA Innovative Advance Concepts
O <sub>2</sub>	Oxygen Gas
PA	Pressure of Internal Atmosphere
PBSA	Pressure Applied to surface by Mass
PFSA	Pressure Applied by Feet
PROB	Likelihood
RM	Risk Management
RMP	Rotation Motion Profile
RPN	Risk Priority Number
SEV	Severity
TBD	To be Determined
TRL	Technology Readiness Level

## Nomenclature

$t_{ar}$	= Time Duration of the Acceleration Sub-Phase of Rotation
$t_{cr}$	= Time Duration of the Constant Spin Sub-Phase of Rotation
$t_{dr}$	= Time Duration of the Deceleration Sub-Phase of Rotation
$\alpha$	= Angular Acceleration
$\alpha_{ar}$	= Angular Acceleration during Acceleration Sub-Phase of Rotation
$\alpha_{cr}$	= Angular Acceleration during Constant Spin Sub-Phase of Rotation
$\alpha_{dr}$	= Angular Acceleration during Deceleration Sub-Phase of Rotation
$\theta_{ar}$	= Angle Traveled during Acceleration Sub-Phase of Rotation
$\theta_{cr}$	= Angle Traveled during Constant Spin Sub-Phase of Rotation
$\theta_{dr}$	= Angle Traveled during Deceleration Sub-Phase of Rotation
$\omega$	= Rotation Spin Rate
$\omega_{ar}$	= Rotation Spin Rate during Acceleration Sub-Phase of Rotation
$\omega_{cr}$	= Rotation Spin Rate during Constant Spin Sub-Phase of Rotation
$\omega_{dr}$	= Rotation Spin Rate during Deceleration Sub-Phase of Rotation

$\Delta h$	=	Minimum Crash Distance
$\Delta K$	=	Kinetic Energy
$\Delta P$	=	Potential Energy
$a$	=	Acceleration (Earth Gravity 9.81 m/s <sup>2</sup> )
$A$	=	Cross Section of Tibia
$a_{cent}$	=	Centripetal Acceleration
$a_{tan}$	=	Tangential Acceleration
$B$	=	Block Number
$D$	=	Difficulty of Production
$D$	=	Distance from the Glabella (between the eyes) to Top of Head
$F_{Cent}$	=	Centripetal Inertial Force
$F_{lin}$	=	Linear Inertial Force
$F_t$	=	Tangential Inertial Force
$F_{end}$	=	Force at the End of the Track
$H$	=	Height of Astronaut
$L$	=	Distance from the Center of the Head to the Bottom of feet of an Astronaut
$L_{track}$	=	Length of Segment of the Track
$M$	=	Total Dry Mass of the System
$M$	=	Combine Mass of Pod, Astronaut and Counter Balance
$m$	=	Mass of Astronaut
$M_{track}$	=	Mass of Track
$P$	=	Maximum Pressure applied before Tibia's Fracture
$P_L$	=	Power of Linear Phase
$P_R$	=	Power of Rotation Phase
$Q$	=	Production Quantity
$r$	=	Distance from the Glabella to Center of the Mass of an Astronaut
$S$	=	Specification Value – Human Habitat is 2.13
$t$	=	Time at the Location
$T$	=	1-Track Period
$T_a$	=	Linear Acceleration Duration
$T_d$	=	Linear Deceleration Duration
$T_R$	=	Rotation Acceleration Phase Duration
$T_t$	=	Transition Duration
$T_{ta}$	=	Transition Linear Acceleration Duration
$T_{td}$	=	Transition Linear Deceleration Duration
$v$	=	Velocity at the End of Track
$V$	=	Instantaneous Linear Velocity of the Pod
$\rho$	=	Material Density

## References

- <sup>1</sup>Buckey, J. C. *Space Physiology*. New York: Oxford University Press, 2006.
- <sup>2</sup>Clement, G., Buckley, A., and Paloski, W. H. "Artificial Gravity as a Countermeasure for Mitigating Physiological Deconditioning during Long-Duration Space Missions" *Frontiers in Systems Neuroscience* Vol. 9, No. 92. (2015)
- <sup>3</sup>Clement, G., Charles, J., Norsk, P. and Paloski, W.H. "Human Health Counter Measure Element, Artificial Gravity Evidence Report", Version 6. NASA.(2015)
- <sup>4</sup>Clauser, C.E and et al. "Weight, Volume and Center of Mass of Segments of the Human Body." Air Force Systems Command Wright-Patterson Air Force Base, Ohio (1969).
- <sup>5</sup>Vincent, G., et al. "Observer Model Analysis of Orientation Perception during Artificial Gravity Stimulation via Centrifugation versus Linear Sled" 32nd American Society of Gravitational and Space Research Conference. Cleveland, OH. (2016)
- <sup>6</sup>NASA. "International Space Station Familiarization." Mission Operations Directorate, Space Flight Training Division. (1998)
- <sup>7</sup>Seyedmadani, K. et al. "The Linear Sled "Hybrid" Approach for Artificial Gravity as a Countermeasure for Crewed Long Duration Space Exploration Missions." AIAA Space Forum, Conference Paper, Orlando FL. (2017)
- <sup>8</sup>International Space Station Familiarization. Mission Operations Directorate, Space Flight Training Division, NASA.
- <sup>9</sup>Anderson, M. Ewart, M. Keener, J. and Wanger, S (2015) "Life Support Basline Values and Assumptions Document (BVAD)" NASA JSC, Houston, TX.
- <sup>10</sup>Naidoo, N., Lazarus, L., Ajayi, N. O., and Satyapal, K. S. "Anthropometry of the Black Adult Tibia: A South African Study," *International Journal of Morphology* Vol. 33, No. 2, pp. 600-606. (2015)
- <sup>11</sup>Petersen, N., Jaekel, P., Rosenberger, A., Weber, T., Scott, J., Castrucci, F., Lambrecht, G., Ploutz-Snyder, L., Damann, V., Kozlovskaya, I., and Mester, J. "Exercise in space: the European Space Agency approach to in-flight exercise countermeasures for long-duration missions on ISS," *Extreme Physiology & Medicine* Vol. 5.(2016)  
doi: ARTN 9 10.1186/s13728-016-0050-4
- <sup>12</sup>Fairburn, S., and Walker, S. "Sleeping With the Stars - The Design of a Personal Crew Quarter for the International Space Station," *31st International Conference on Environmental Systems*. Orlando, FL. (2001)
- <sup>13</sup>J. Sendroy and H. A. Collison "Determine human body volume" *Journal of Applied Physiology* Vol.21, No. 1. Jan (1966)
- <sup>15</sup>Wieland, "Designing for Human Presence in Space" NASA RP-1324, 1994
- <sup>16</sup> Yu C.-Y., Lin C.-H. & Yang Y.-H. Human body surface area database and estimation formula. *Burns* 36, 616–629 (2010).
- <sup>17</sup>Shavers, M. R., Zapp, N., Barber, R. E., Wilson, J. W., Qualls, G., Toupes, L., Ramsey, S., Vinci, V., Smith, G., and Cucinotta, F. A. "Implementation of ALARA radiation protection on the ISS through polyethylene shielding augmentation of the Service Module Crew Quarters," *Space Life Sciences: Radiation Risk Assessment and Radiation Measurement in Low Earth Orbit* Vol. 34, No. 6 pp. 1333-1337. (2004)  
doi: 10.1016/j.asr.2003.10.051
- <sup>18</sup>Slaba, T. C., Bahadori, A. A., Reddell, B. D., Singleterry, R. C., Cloudsley, M. S., and Blattig, S. R. "Optimal shielding thickness for galactic cosmic ray environments," *Life Sciences in Space Research* Vol. 12, pp. 1-15. doi: 10.1016/j.lssr.2016.12.003-(2017)

<sup>19</sup>Clark, T.K., Seyedmadani, K., and Gruber J. “Turbolift – A Linear Sled Hybrid Approach to Artificial Gravity” (presentation and poster) NASA Innovative and Advanced Concepts Symposium, Denver, CO. (2017)

<sup>20</sup>Larson, W.J., Pranke, L.K. “Human Spaceflight Mission Analysis and Design” *The McGraw-Hill Companies*, Ch 29 page 946.

<sup>21</sup>Jones, W.H. “Estimate the Life Cost of Space Systems” *45<sup>th</sup> International Conformance on Environmental Systems*, Washington. July (2015)

<sup>22</sup>NASA Cost Estimating Handbook, Version 4.0, Pg 14- 23. (2015)

<sup>23</sup>Owens, A. and DeWeck, O. “Sensitivity Analysis of the Advanced Mission Cost Mode;” *46<sup>th</sup> International Conformance on Environmental Systems*, Vienna, Austria. July (2016)

<sup>24</sup>NASA Handbook of Systems Engineering, Version 2.0 Pg160 to 166. (2017)

<sup>25</sup>McDermott, R.E., Mikulak, R.J. and Beauregard, M.R. “The Basic of FMEA” *Quality Recourses*. New York. (1996)

<sup>26</sup>Griffin, B. N. and Dischinger, C. “Low Cost Space Demonstration for a Single-Person Spacecraft” *American Institute for Aeronautics and Astronautics* (2011).

**Appendix**

**Mass and Power Calculation for Overall the LSH System:**

Case RMP	Case LMP	Length (m)	Mass of Track, Pod and Counterweight (Kg)	Average Power (Kw)	Energy Required for the Motion and the Pod Systems (Kw-Hr)
<b>A</b>	1	43.98	6144.93	10.7034	7535.05
	2	25.36	3677.11	10.7034	12368.53
	3	6.95	1237.12	4.9782	11092.36
<b>B</b>	1	45.58	6356.99	10.6845	7304.06
	2	25.85	3742.05	10.6845	11771.87
	3	7.32	1286.16	3.6009	7333.91
<b>C</b>	1	49.46	6871.23	7.7205	4901.19
	2	29.84	4270.87	7.7205	7567.38
	3	8.32	1418.70	2.1185	3510.61
<b>D</b>	1	47.29	6583.62	9.1135	6030.34
	2	27.58	3971.34	9.1135	9531.24
	3	7.75	1343.15	2.7460	5090.02

**Power for one-cycle of the LSH system (using LMP #2):**

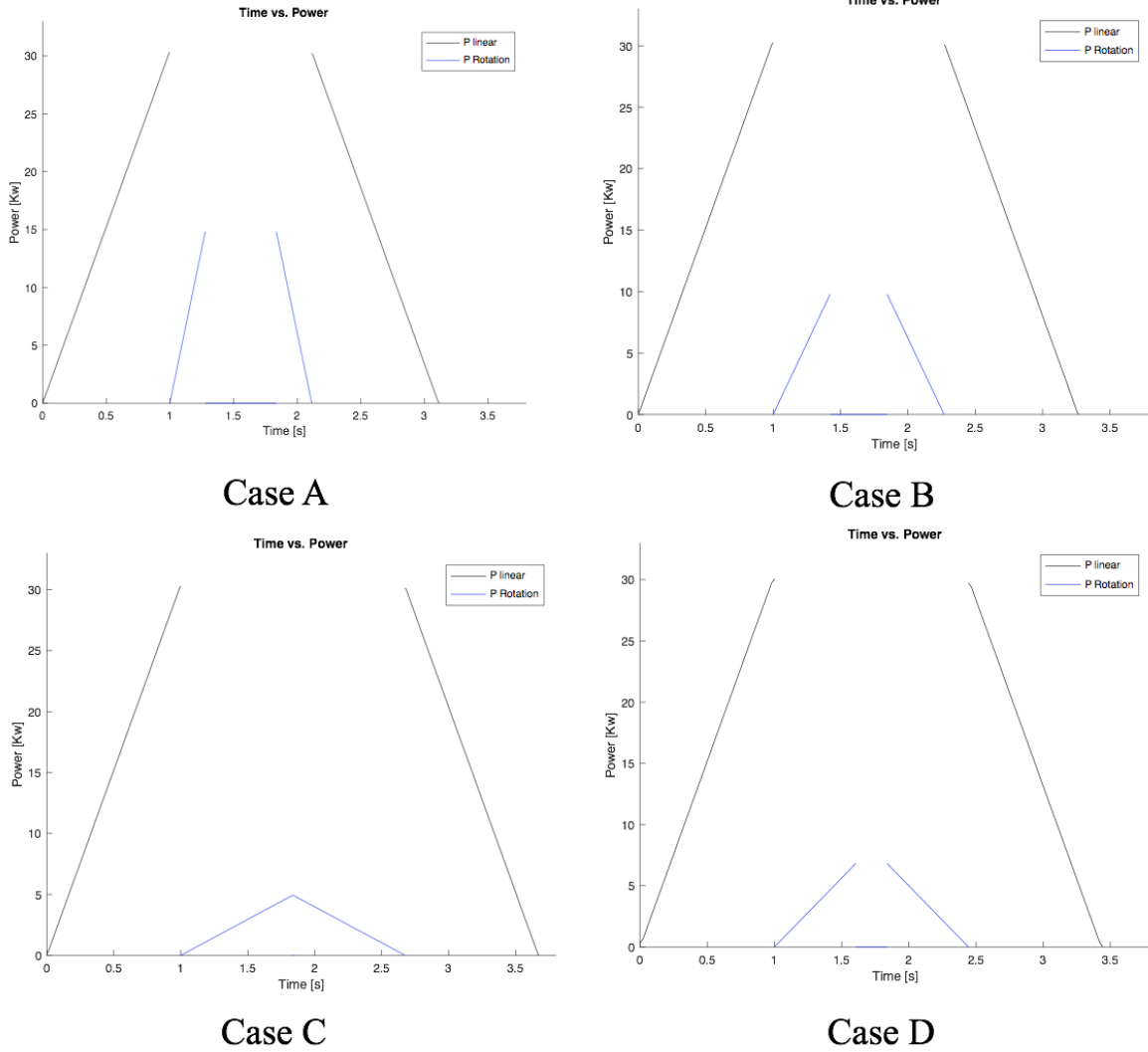


Figure 16: Power for one-cycle for LMP 2

## Risk Definitions

<b>Refer to Risk Management Plan</b>			
Statement	<i>Given that CONDITION, there is the possibility that DEPARTURE, resulting in CONSEQUENCE.</i>		
Mitigation Cost	Money/Schedule		
Area of Impact	Mission/Payload/Subsystem/Spacecraft, etc...		
Class	Technical/Mission/Programmatic/Cost/Safety		
Likelihood	<b>Likelihood</b>	<b>Likelihood of Risk Occurrence</b>	<b>... or – The current process ...</b>
	1	Extremely Remote	is sufficient to prevent this event
	2	Unlikely	will most likely prevent this event
	3	Possible	may prevent this event but additional actions will be required
	4	Likely	cannot prevent this event but a different approach or process might
	5	Highly Likely	cannot prevent this event and no alternative approaches or processes are available
Consequence	Refer to Risk Management Plan		
Timeframe	Near-term: TRL 1-2 - NIAC Phase I and Phase II Mid-term: TRL 3-5 - Next 15 Years Long-term: TRL 6-9 Next 25 years		
Board Action	RESEARCH - Gather more information about it. WATCH - Identify "triggers" before taking any action about the risk. MITIGATE - Reduce, eliminate, or avoid the risk.		
Risk Action	Research - Gather more information about it. Watch - Identify "triggers" before taking any action about the risk. Mitigate - Reduce, eliminate, or avoid the risk. Reject - It is determined that it has no impact to the Program or if it can be resolved at a lower level		

Risk Data Base

Risk ID	1	Title	Gravity Variation
Statement	Damage to Components	Area of Impact	Technology
Context		Class	Programmatic
Mitigation plan		Consequence	4
Mitigation Cost		Likelihood	2
Timeframe	Long-term	Score	8
Risk Action	Mitigate	Board Action	approved

Risk ID	2	Title	Vibration
Statement	Vibration - During Launch	Area of Impact	Technology
Context		Class	Mission
Mitigation plan	better understanding on our	Consequence	4
Mitigation Cost		Likelihood	3
Timeframe	long term	Score	12
Risk Action	Mitigate	Board Action	approved

Risk ID	3	Title	Development
Statement	Loss of Launch	Area of Impact	Technology
Context		Class	Mission
Mitigation plan		Consequence	5
Mitigation Cost		Likelihood	2
Timeframe	Long term	Score	10
Risk Action	Watch	Board Action	approved

Risk ID	4	Title	Assembly
Statement	Assembly	Area of Impact	Structure or Pod
Context	during solar flare	Class	Operations
Mitigation plan	having timely safe modes	Consequence	5
Mitigation Cost	failure of system	Likelihood	3
Timeframe	Long-term	Score	15
Risk Action	Watch	Board Action	approved

Risk ID	5	Title	Stop at end
Statement	failure to stop at end	Area of Impact	Track / craft
Context	during mission	Class	operations
Mitigation plan	- built in factor of safety	Consequence	2
Mitigation Cost	potential failure of mission	Likelihood	5
Timeframe	Long-term	Score	10
Risk Action	Watch	Board Action	approved

Risk ID	6	Title	ECLSS
Statement	Pod - ECLSS Leak	Area of Impact	Space craft
Context	Life support	Class	programmatic
Mitigation plan	monthly meeting	Consequence	3
Mitigation Cost	secondary resource	Likelihood	2
Timeframe	Mid-term	Score	6
Risk Action	Watch	Board Action	approved

Risk ID	7	Title	Radiation
Statement	Pod communication effect	Area of Impact	Pod
Context	during testing, safety issues, overworking during entire project	Class	programmatic
Mitigation plan	secondary system	Consequence	4
Mitigation Cost	time and financial	Likelihood	4
Timeframe	Mid-term	Score	16
Risk Action	Discussions	Board Action	approved
Risk ID	8	Title	Fire
Statement	Electrical - fire	Area of Impact	Pod
Context	electric fire in the cabin	Class	programmatic
Mitigation plan	concentration of O2 <30%	Consequence	3
Mitigation Cost	pressurize volume	Likelihood	1
Timeframe	mid-term	Score	3
Risk Action	calculation	Board Action	
Risk ID	9	Title	Connectors
Statement	Connecting to airlock	Area of Impact	Airlock
Context	staying more than 1 hr. in the pod	Class	Operations
Mitigation plan	redundancy	Consequence	4
Mitigation Cost	redundancy in resources	Likelihood	3
Timeframe	mid- term and near-term	Score	12
Risk Action		Board Action	
Risk ID	10	Title	Power Failure
Statement	Power failure due to radiation or technology failure	Area of Impact	LSH - Actuators
Context	staying more than 1 hr. in the pod	Class	Operations
Mitigation plan	watchdog and report to space craft	Consequence	4
Mitigation Cost	redundancy in resources	Likelihood	3
Timeframe	mid- term and near-term	Score	12
Risk Action		Board Action	
Risk ID	11	Title	Actuator Out of Railing
Statement	on railing due to structure Failure	Area of Impact	LSH - Actuators
Context		Class	Operations
Mitigation plan	structural analysis and guide railing	Consequence	4
Mitigation Cost	material and structure	Likelihood	4
Timeframe	mid- term and near-term	Score	16
Risk Action		Board Action	